Local-phonon model of strong electron-phonon interactions in $A15$ compounds and other strong-coupling superconductors

Clare C. Yu and P. W. Anderson
Physics Department, Princeton University, Princeton, New Jersey 08544
and AT&T Bell Laboratories, Murray Hill, New Jersey 07974
(Received 28 November 1983)

We propose a model in which a single atom interacts strongly with a Fermi gas of spinless electrons. We find that the electrons provide an effective double-well potential for the atom. The electron-phonon coupling Λ is renormalized downward with decreasing temperature, provided that Λ is large at high temperatures. The model is consistent with the experimental temperature dependence of the Pauli susceptibility and the resistivity as well as with the violation of Mattheissen's rule. It provides a possible explanation for why the observed martensitic transition is so small. We find that the violation of Migdal's theorem implies time-retarded interactions between hops of the atom from one minimum of the double well to the other.

I. INTRODUCTION

The $A15$ compounds have long been known to have a puzzling array of physical properties.[1] Members of this group have high superconducting transition temperatures indicative of strong electron-phonon coupling. The "saturation" of the resistivity with increasing temperature implies that strong electron-phonon scattering has reduced the electron mean free path to the order of the lattice spacing.[2] In addition, it appears that Mattheissen's rule is violated in these materials. There is also evidence for anomalously large zero-point motion as well as anharmonicity.[3,4] In fact the shear-mode elastic constant $(C_{11}-C_{12})/2$ in V_3Si softens with decreasing temperature.[5] Yet, even though phonon softening is seen at temperatures on the order of the Debye temperature Θ_D, the martensitic transition occurs at very low temperatures ($T_m \sim 21$ K in V_3Si) if it occurs at all. Furthermore, the lattice displacements associated with this structural transition are less than 0.01 Å. This is about 10 times less than a typical thermal or zero-point fluctuation, ~ 0.1 Å. Studies of the specific heat indicate that the density of states at the Fermi surface $N(0)$ is large, e.g., in V_3Si, $\gamma = 52.8$ mJ/mol K^2 implies $N(0) \sim 2.4$ states/eV atom.[6] The Knight shift and susceptibility have been found to be strongly temperature dependent for alloys with high superconducting transition temperatures.[7] In particular, the susceptibility increases as the temperature decreases.

Previous theories have attributed these properties to a peak in the density of states at the Fermi surface,[1] anharmonic phonons,[8] and the one dimensionality of the chains of A atoms in A_3B compounds.[9] In this paper we propose a model in which a single atom on the chain interacts strongly with a Fermi gas of electrons. We consider one mode of vibration of the atom, possibly along the direction of the chain. Neighboring atoms provide an electrostatic restoring force which tends to be screened by the cloud of electrons. This reduces the bare phonon frequency and softens the lattice. If we increase the electron-phonon coupling sufficiently, a simple harmonic potential well will deform into a double well. It may seem odd to replace the $A15$ compounds by one atom. However, if the electron-phonon coupling is very large, each atom will interact much more with the electrons surrounding it than with neighboring atoms. This approximation is clearly even more justifiable in other strong-coupling superconductors with similar properties such as the Chevrel compounds.[10]

In Sec. II we use Tomonoga bosons to show how strong electron-phonon coupling can lead to anharmonic phonons. In Sec. III we present the Hamiltonian for the local phonon. We then proceed in Sec. IV to integrate out the electrons and to find an effective double-well potential for the atom. We shall see that a consequence of violating Migdal's theorem is time-retarded interactions between hops from one minimum to the other. In Sec. V we apply space-time scaling techniques to show that, if the system starts with large electron-phonon coupling λ at high temperatures, λ is renormalized downwards as the temperature is decreased. This is reflected in the downward renormalization of the phase shift and the increase in the tendency for hopping. Essentially the double well becomes shallower and gradually transforms into a single well. In Sec. VI we discuss specific heat and susceptibility. In particular, we show that our model is consistent with experimental data on the temperature dependence of the Pauli susceptibility at high temperatures. In Secs. VII and VIII we compare the prediction of the local phonon picture with the temperature dependence of the resistivity for $T \gtrsim \Theta_D$ and with the violation of Mattheissen's rule. We deal with the physical meaning of the increase in the tendency for hopping with decreasing temperature in Sec. IX, and we relate this to why the observed martensitic transition is so small in Sec. X. Concluding remarks are contained in Sec. XI.

II. TOMONOGA BOSONS

Tomonoga bosons provide a more precise way of seeing the interplay between large resistivity and anharmonic phonons.[11,12] Consider for the moment a spherical shell of atoms or positively charged ions which are surrounding

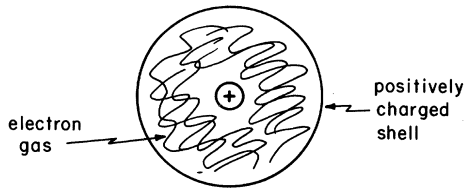

FIG. 1. Tomonoga bosons correspond to radial density waves in the electron gas.

an electron gas as shown in Fig. 1. In the center of the sphere sits our atom of interest. Suppose the shell vibrates radially. Radial density waves in the electron gas will result. The quantized version of these s waves are Tomonoga bosons. We can consider a one-dimensional problem because we are just dealing with the radial coordinate.

The electron-phonon Hamiltonian can be written

$$H_{\text{el-ph}}=\lambda Q \sum_{\vec{k},\vec{k}'} c^{\dagger}_{\vec{k}} c_{\vec{k}'} , \tag{1}$$

where Q is the radial displacement and $c_{\vec{k}}$ is an electron annihilation operator. The electron-phonon coupling λ can be written, in terms of a dimensionless parameter Λ, as

$$\lambda^2=\frac{M\omega_0^2}{2\pi N(0)}\Lambda^2 , \tag{2}$$

where M is the mass of the shell, ω_0 is the bare phonon frequency, and $N(0)$ is the density of electron states of one spin at the Fermi level in one dimension. Λ is the analogue of Migdal's λ_0 in that $\Lambda \lesssim 1$ for ordinary metals. A typical value for Λ is 0.2. We cannot use Migdal's parameter because that was derived for acoustic phonons. We can write Eq. (1) in terms of Tomonoga bosons by introducing the density operators

$$\rho^{\pm}_k=\frac{1}{\sqrt{L}}\sum_{\pm q>0} c^{\dagger}_{q-k/2}c_{q+k/2} ,$$

where L is the length of the system. It is of the order of the lattice constant. The Tomonoga boson creation and annihilation operators are given by

$$a_k=\left[\frac{2\pi}{|k|}\right]^{1/2}\times\begin{cases}\rho^{+}_{\vec{k}}, & k>0\\ \rho^{-}_{\vec{k}}, & k<0\end{cases}$$

$$a_k=\left[\frac{2\pi}{|k|}\right]^{1/2}\times\begin{cases}\rho^{+}_{k}, & k>0\\ \rho^{-}_{k}, & k<0\end{cases}$$

$$[a_k,a_{k'}]=0, \quad [a_k,a^{\dagger}_{k'}]=\delta_{kk'} .$$

Then Eq. (1) becomes

$$H=\sum_{|k|<k_c}\Omega_k a^{\dagger}_k a_k+\omega_0 b^{\dagger}b + \sum_{|k|<k_c}\frac{\Lambda}{4}\left[\frac{\omega_0\Omega_k}{2\pi}\right]^{1/2}(b+b^{\dagger})(a^{\dagger}_k+a_{-k}) , \tag{3}$$

where we used

$$Q=\left[\frac{1}{2M\omega_0}\right]^{1/2}(b+b^{\dagger})$$

and

$$N(0)=L/\pi v_F .$$

As Tomonoga showed in his original paper, $\Omega_k=v_F|\vec{k}|$. We assume that the electron density varies smoothly within the density waves. These long-wavelength variations are why we introduce a cutoff wave vector $k_c<k_F$. The phonon creation and annihilation operators associated with the shell vibrations are given by b and $b^{\dagger}$. Since H is quadratic, we can solve it exactly. We introduce phonon and Tomonoga boson fields as

$$\phi=\frac{1}{\sqrt{2}}(b+b^{\dagger})$$

$$\psi_k=\frac{1}{\sqrt{2}}(a_k+a^{\dagger}_k)$$

$$H=\sum_{|k|<k_c}\Omega_k a^{\dagger}_k a_k+\omega_0 b^{\dagger}b + \sum_{|k|<k_c}\frac{\Lambda}{2}\left[\frac{\omega_0\Omega_k}{2\pi}\right]^{1/2}\phi\psi_k . \tag{4}$$

The retarded Green's functions associated with these fields in the Heisenberg representation are

$$D_R(t)=-i\Theta(t)\langle 0|[\phi(t),\phi(0)]|0\rangle ,$$

$$G_R(k;t)=-i\Theta(t)\langle 0|[\psi_k(t),\phi(0)]|0\rangle .$$

We can calculate the phonon self-energy using the equation-of-motion method. When we do so, we find

$$\Pi_R(\omega)=\frac{v_F k_c x}{2}\left[\omega\ln\left|\frac{\omega+v_F k_c}{\omega-v_F k_c}\right|-2v_F k_c\right]-i\pi v_F k_c x\omega , \tag{5}$$

where $x=(\Lambda^2\omega_0^2 L)/(8\pi^2 v_F^2 k_c)$ is dimensionless. The full phonon propagator is given by

$$D_R(\omega)=\frac{\omega_0}{\omega^2-\omega_0^2-\Pi_R(\omega)} . \tag{6}$$

The real part of $\Pi_R(\omega)$ is related to the phonon frequency shift, while the imaginary part gives the phonon decay rate. Since the phonons decay by scattering off the Tomonoga bosons, the imaginary part is a measure of the electron scattering rate and, hence, of the resistivity. Even though the decay rates of electrons and phonons are not the same, the resistivity of the $A15$ compounds is so large at $T\sim\Theta_D$ that we expect the phonon decay rate Γ to also be large. From the poles of $D_R(\omega)$ we see that the decay rate is

$$\Gamma=\frac{\pi v_F k_c x}{2(1-x)} , \tag{7}$$

and the renormalized frequency is

$$\omega'=\frac{[(\omega_0^2-v_F^2k_c^2x)(1-x)-(\frac{1}{2}\pi v_F k_c x)^2]^{1/2}}{1-x} , \tag{8}$$

since $\omega \ll v_F k_c$. Lattice stability requires that the discriminant be positive and this in turn puts an upper bound on Λ^2. The critical coupling Λ_c is given by $\omega'=0$. If $k_c=\frac{1}{2}k_F$,

$$\Lambda_c \simeq 4\pi/k_F L \ . \tag{9a}$$

Inserting Λ_c into our expression for Γ gives us the maximum allowed decay rate:

$$\frac{\Gamma_{\max}}{\omega_0} \simeq \pi(\omega_0/E_F) \ll 1 \ . \tag{9b}$$

If $\omega_0 \sim \omega_D$, the critical decay rate is small, much smaller than what is implied by the large resistivity of the $A15$ compounds, but if we let Λ exceed Λ_c to increase the decay rate, the phonon will go soft and become unstable unless ω_0 is very large, i.e., unless the phonon has a large intrinsic stiffness.

Such a large electron-phonon coupling implies that Migdal's theorem will be violated.[13] Among other things, Migdal's theorem tells us that electron-phonon vertex corrections will be of the order of $N(0)g^2/\omega_D(m/M)^{1/2}$ where m is the mass of the electron, M is the mass of the ion, and ω_D is the Debye frequency. g is a coupling energy. In our notation we can take $g^2 \sim \hbar\lambda^2/M\omega \sim \Lambda^2\hbar\omega/2\pi N(0)$. In normal metals $N(0)g^2/\omega_D$ is of the order of unity. Thus, lowest-order perturbation theory is sufficient if we include Coulomb corrections. This is the basis of the Eliashberg equations. If g is roughly an order of magnitude larger than normal, perturbation theory does not hold, i.e., free electrons and free phonons are not a good zeroth-order approximation and are not the proper starting point in Hilbert space. In essence, Migdal's theorem is a restatement of the adiabatic approximation which assumes that one can separate the electrons from the phonons and that the electrons are always in equilibrium with the phonons. We shall see that the violation of Migdal's theorem implies that there are time-retarded interactions between the electrons which are mediated by the phonons.

III. HAMILTONIANS

Let us now return to our model in which we approximate the optical phonons by independent Einstein oscillators. We consider an ion moving back and forth about its lattice site in one dimension and interacting with an electron gas. Obviously, it will make no difference if the ion is displaced to the right or to the left, and the Hamiltonian must preserve this symmetry. We can imagine expanding the electron wave functions in spherical harmonics about the lattice site. Denoting the atomic displacement by Q, the Hamiltonian must be invariant under the transformations $Q \to -Q$, s wave$\to s$ wave, and p wave$\to -p$ wave. Rather than a partial-wave analysis, we can separate the wave function into two parts with even and odd parity.

The Hamiltonian is

$$H = H_{\rm ph} + H_{\rm el} + H_{\text{el-ph}} \ ,$$

where

$$H_{\rm ph} = \frac{P^2}{2M} + \tfrac{1}{2}M\Omega^2 Q^2 \ , \tag{10a}$$

$$H_{\rm el} = \sum_{\vec{k}} \epsilon_{\vec{k}s} c^\dagger_{\vec{k}s} c_{\vec{k}s} + \sum_{\vec{k}} \epsilon_{\vec{k}p} c^\dagger_{\vec{k}p} c_{\vec{k}p} \ , \tag{10b}$$

$$H_{\text{el-ph}} = -\sum_{\vec{k},\vec{k}'} (c^\dagger_{\vec{k}'s} \ \ c^\dagger_{\vec{k}'p}) \begin{pmatrix} 0 & \lambda Q \\ \lambda Q & 0 \end{pmatrix} \begin{pmatrix} c_{\vec{k}s} \\ c_{\vec{k}p} \end{pmatrix} . \tag{10c}$$

As before we can express the coupling in terms of a dimensionless parameter Λ,

$$\lambda^2 = \frac{M\Omega^2}{2\pi N(0)}\Lambda^2 \ , \tag{11}$$

where $N(0)$ is the density of states at the Fermi surface for one type of electron. The minus sign in $H_{\text{el-ph}}$ ensures that the interaction between the electrons and the atom is attractive. This term represents the fact that the phonon scatters even-parity electrons into odd-parity electrons and vice versa. The diagonal matrix elements have been absorbed into $H_{\rm el}$. P and M denote the atomic momentum and mass, respectively. $c^\dagger_{\vec{k}s}, c_{\vec{k}s}$ are the creation and annihilation operators for the even-parity electrons of wave vector $\vec{k}$, and $c^\dagger_{\vec{k}p}, c_{\vec{k}p}$ are the analogous operators for odd-parity electrons. Under a parity transformation, $c_{\vec{k}s} \to c_{\vec{k}s}$ and $c_{\vec{k}p} \to -c_{\vec{k}p}$. $\epsilon_{\vec{k}s}$ and $\epsilon_{\vec{k}p}$ are the electron energies and can be approximated by $v_F|\vec{k}|$. For simplicity we will assume that $\epsilon_{\vec{k}s} = \epsilon_{\vec{k}p} = \epsilon_k$. In principle, this does not affect anything; actually, the Fermi velocity will be anisotropic and both the "s" and "p" waves will propagate aspherically. With this assumption we can diagonalize the Hamiltonian by transforming to the basis

$$c_{\vec{k}\pm} = \frac{1}{\sqrt{2}}(c_{\vec{k}s} \pm c_{\vec{k}p}) \ .$$

Then the Hamiltonian becomes

$$H_{\rm el} = \sum_{\substack{\vec{k}, \\ \sigma=\pm}} \epsilon_k c^\dagger_{\vec{k}\sigma} c_{\vec{k}\sigma} \ ,$$

$$H_{\text{el-ph}} = -\sum_{\vec{k},\vec{k}'} (c^\dagger_{\vec{k}'+} \ \ c^\dagger_{\vec{k}'-}) \begin{pmatrix} \lambda Q & 0 \\ 0 & -\lambda Q \end{pmatrix} \begin{pmatrix} c_{\vec{k}+} \\ c_{\vec{k}-} \end{pmatrix} . \tag{12}$$

A physically equivalent Hamiltonian has the form of the Anderson model for localized magnetic moments.[14] We can imagine an electron localized in the vicinity of the atom. This electron, which has creation and annihilation operators $\psi^\dagger_{0\pm}$ and $\psi_{0\pm}$, mixes with the conduction-band electrons via the transition matrix $V_{\vec{k}0}$. Thus we can write

$$H_{\rm el} = \sum_{\substack{\vec{k}, \\ \sigma=\pm}} \epsilon_k c^\dagger_{\vec{k}\sigma} c_{\vec{k}\sigma} + \sum_{\sigma=\pm} E_0 \psi^\dagger_{0\sigma}\psi_{0\sigma} + \sum_{\vec{k},\sigma} (V_{\vec{k}0} c^\dagger_{\vec{k}\sigma}\psi_{0\sigma} + V^*_{\vec{k}0}\psi^\dagger_{0\sigma} c_{\vec{k}\sigma}) \ , \tag{13}$$

$$H_{\text{el-ph}} = -(\psi^\dagger_{0+} \ \ \psi^\dagger_{0-}) \begin{pmatrix} \lambda Q & 0 \\ 0 & -\lambda Q \end{pmatrix} \begin{pmatrix} \psi_{0+} \\ \psi_{0-} \end{pmatrix} , \tag{14}$$

where the $\pm$ subscripts denote symmetric and antisym-

metric combinations of s and p waves. E_0 is the energy of the unperturbed local electron state. If $\lambda=0$, $H_{\rm el}$ in Eq. (13) should be equivalent to the "free-band" Hamiltonian in Eq. (12). In this case the localized electron state is entirely fictitious and there should be maximum mixing with the band electrons. The width of the resonance $\Delta=\pi N(0)|V_{\vec{k}0}|^2$ is on the order of the bandwidth. In other words, if we put an electron on the lattice site, it will decay away by mixing with the band electrons and its lifetime $\tau\sim 1/\Delta$. In terms of Δ and the dimensionless parameter Λ, λ can be expressed as

$$\lambda^2=\frac{\pi M\Omega^2\Delta}{2}\Lambda^2 . \tag{15}$$

In this form it is easy to see the relation between our model and the Jahn-Teller effect.[15] Suppose we ignore the band electrons and set $E_0=E_F=0$. Then $H_{\rm el}=0$ in Eq. (13) and the full Hamiltonian becomes

$$H=\frac{P^2}{2M}+\tfrac{1}{2}M\Omega^2Q^2-\lambda Q\psi_{0+}^\dagger\psi_{0+}+\lambda Q\psi_{0-}^\dagger\psi_{0-} . \tag{16}$$

Letting $n_{0\pm}=\psi_{0\pm}^\dagger\psi_{0\pm}$ and completing the square in Q, we obtain

$$H=\frac{P^2}{2M}+\tfrac{1}{2}M\Omega^2x^2-\frac{\lambda^2}{2M\Omega^2}(n_{0+}-n_{0-})^2 ,$$

where

$$x=Q-\frac{\lambda}{M\Omega^2}(n_{0+}-n_{0-}) . \tag{17}$$

If $n_{0+}=n_{0-}$, $Q=0$ is stable. But if $n_{0+}=1$ and $n_{0-}=0$, the minimum of the potential is displaced to

$$Q_{0+}=\lambda/M\Omega^2 . \tag{18}$$

We can express Q in terms of a dimensionless parameter q as follows:

$$Q^2=q/M\Omega . \tag{19}$$

We can think of q as the number of phonons present, although q is not necessarily an integer. Thus Q_0 corresponds to

$$q_0=\pi\Lambda^2\Delta/2\Omega .$$

Noting that $n_{0\pm}^2=n_{0\pm}$, we can identify the coefficient of $n_{0\pm}$ to be $E'_{0\pm}$. Then E'_{0+} is lower relative to E'_{0-} by

$$-\delta E'=-\lambda^2/2M\Omega^2=-\tfrac{1}{2}\Omega q_0 . \tag{20}$$

Similarly, if $n_{0+}=0$ and $n_{0-}=1$, the atom moves in the other direction. Thus we have the Jahn-Teller effect; namely, the system is unstable to a distortion which splits the degeneracy between the local "+" and "−" electron levels. Tunneling between Q_{0+} and Q_{0-} leads to the dynamic Jahn-Teller effect.

IV. PATH-INTEGRAL FORMULATION

Since the Anderson-model Hamiltonian in Eqs. (13) and (14) gives the same physics as the "free-band" Hamiltonian in Eq. (12), it does not matter which we choose to study. We will concentrate our efforts on the free-band Hamiltonian and occasionally cite the analogous results for the Anderson model. We start by integrating out the fermions using path-integral techniques similar to those used by Yuval and Anderson on the Kondo problem,[16] and by Hamann[17] on the Anderson model of localized moments. This will produce an effective double-well potential for the atom as well as a retarded interaction between hops from one well to the other. We can then write the partition function in a form similar to that found by Yuval and Anderson for the Kondo problem and apply space-time scaling techniques[18] to derive scaling relations for the scattering phase shift and hopping fugacity.

The partition function can be expressed as

$$Z=Z_0\left\langle T_\tau\exp\left[-\int_0^\beta d\tau H_I(\tau)\right]\right\rangle ,$$

where Z_0 is the partition function for $H_0=H_{\rm el}$, H_I is in the interaction representation defined by H_0, T_τ is the ordering operator with respect to τ, and $\langle\ \rangle$ is the thermal average with respect to H_0. H_I is given by $H_{\text{el-ph}}$ in Eq. (12). This yields

$$Z=Z_0Z_+Z_- , \tag{21}$$

where

$$Z_\sigma=\left\langle T_\tau\exp\left[-\sum_{\vec{k},\vec{k}'}\int_0^\beta d\tau E_\sigma(Q(\tau))c_{\vec{k}'\sigma}^\dagger(\tau)c_{\vec{k}\sigma}(\tau)\right]\right\rangle ,$$

$$E_\sigma(Q(\tau))=-\sigma\lambda Q(\tau) \tag{22}$$

$$=-\sigma\left[\frac{M\Omega^2}{\pi N(0)}\right]^{1/2}\Lambda Q ,$$

and

$$\sigma=\pm .$$

We will integrate out the fermions for a fixed path $Q(\tau)$ and then integrate over all paths $Q(\tau)$. For a partition function these paths must be closed, i.e., $Q(0)=Q(\beta)$. Although we should fix the end points, integrate over all paths between these end points, and then vary the end points, we will only consider $Q(0)=Q(\beta)=0$. As Hamann has shown, this constraint does not seriously alter the physics near $T=0$. To evaluate the average in Eq. (22), we follow Hamann and multiply $E_\sigma(Q)$ by a coupling constant g. Differentiating with respect to g, we find

$$\frac{d\ln Z_\sigma}{dg}=-\sum_{\vec{k},\vec{k}'}\int_0^\beta d\tau E_\sigma(Q(\tau))\langle c_{\vec{k}'\sigma}^\dagger(\tau)c_{\vec{k}\sigma}(\tau)\rangle_g , \tag{23}$$

where for any operator A_σ

$$\langle A_\sigma\rangle_g=\frac{\left\langle T_{\tau'}A_\sigma\exp\left[-g\sum_{\vec{k},\vec{k}'}\int_0^\beta d\tau' E_\sigma(Q(\tau'))c_{\vec{k}'\sigma}^\dagger(\tau')c_{\vec{k}\sigma}(\tau')\right]\right\rangle}{\left\langle T_{\tau'}\exp\left[-g\sum_{\vec{k},\vec{k}'}\int_0^\beta d\tau' E_\sigma(Q(\tau'))c_{\vec{k}'\sigma}^\dagger(\tau')c_{\vec{k}\sigma}(\tau')\right]\right\rangle} . \tag{24}$$

The average $\langle c^{\dagger}_{\vec{k}',\sigma}(\tau)c_{\vec{k}\sigma}(\tau)\rangle_g$ is the $\tau'\to\tau^+$ limit of a mixed propagator,

$$G_{\vec{k}\vec{k}',\sigma}(\tau,\tau')=-\langle T_\tau c_{\vec{k}\sigma}(\tau)c^{\dagger}_{\vec{k}',\sigma}(\tau')\rangle_g , \tag{25}$$

which satisfies Dyson's equation. Integrating Eq. (23) gives

$$Z_\sigma=\exp\left[-\int_0^1 dg\int_0^\beta d\tau E_\sigma(Q(\tau))G_\sigma(\tau,\tau^+)\right] , \tag{26}$$

where

$$G_\sigma(\tau,\tau')=\sum_{\vec{k},\vec{k}'}G_{\vec{k}\vec{k}',\sigma}(\tau,\tau') . \tag{27}$$

$G_\sigma(\tau,\tau')$ satisfies Dyson's equation,

$$G_\sigma(\tau,\tau')=G^{(0)}_\sigma(\tau-\tau')+g\int_0^\beta d\tau'' G^{(0)}_\sigma(\tau-\tau'')E_\sigma(Q(\tau''))G_\sigma(\tau''-\tau') . \tag{28}$$

We can find a closed form for $G_\sigma(\tau,\tau')$ by using the "trick" of Nozières and De Dominicis in which the free-electron Green's function is replaced by the function it approaches asymptotically at large times.[19] Dyson's equation then becomes a singular integral equation of the type solved by Muskhelishvili.[20]

The free propagator has the form

$$G^{(0)}_\sigma(\tau)=\begin{cases}-\sum_k e^{-\epsilon_k\tau}[1-f(\epsilon_k)], & \tau>0\\ \sum_k e^{-\epsilon_k\tau}f(\epsilon_k), & \tau<0\end{cases}$$

$$\to\int_{-\infty}^{\infty}d\epsilon N(\epsilon)e^{-\epsilon\tau}[f(\epsilon)-\Theta(\tau)]u(\epsilon) , \tag{29}$$

where $N(\epsilon)$ is the density of states for + or − electrons, $f(\epsilon)$ is the Fermi function, and $u(\epsilon)$ is a cutoff function, e.g.,

$$u(\epsilon)=e^{-|\epsilon|/\xi_0}\ \text{with}\ \xi_0\sim\text{bandwidth} . \tag{30}$$

For long times $\tau\gg 1/\xi_0$, $G^{(0)}_\sigma(\tau)$ becomes

$$G^{(0)}_\sigma(\tau)=-\frac{N(0)}{\tau+(1/\xi_0)\mathrm{sgn}\tau}\simeq-\frac{N(0)}{\tau} , \tag{31}$$

where we have taken $f(\epsilon)$ to be a step function, i.e., we have set $T=0$. We can treat the $\tau=0$ singularity by requiring that the integral

$$\int_{-\alpha}^{\alpha}d\tau G^{(0)}_\sigma(\tau)\ \text{ where } \alpha\gg 1/\xi_0$$

give the same result for the asymptotic form of $G^{(0)}_\sigma(\tau)$ as for the exact form. Doing so, we find that we can take the asymptotic propagator to be

$$G^{(0)}_\sigma(\tau)=-N(0)\left[\mathrm{P}\left[\frac{1}{\tau}\right]+\pi\tan\theta\delta(\tau)\right] , \tag{32}$$

where

$$N(0)\tan\theta=\frac{1}{\pi}\int_{-\infty}^{\infty}d\epsilon N(\epsilon)u(\epsilon)\mathrm{P}\left[\frac{1}{\epsilon}\right] , \tag{33}$$

and P means principal value. Approximation (32) is central to our calculation. It is asymptotically exact for long time intervals. For short time intervals, it is wrong; in the $\tau\to 0$ limit, it leads to spurious divergences in the full propagator $G_\sigma(\tau)$ because we have ignored the cutoff ξ_0. We can handle such divergences by introducing a bandwidth cutoff. We assume that $N(\epsilon)u(\epsilon)$ is symmetric about $\epsilon_F=0$ so that $\tan\theta=0$. Inserting (32) into Dyson's equation (28), we obtain

$$G_\sigma(\tau,\tau')=-N(0)\mathrm{P}\left[\frac{1}{\tau-\tau'}\right]-gN(0)\int_0^\beta\mathrm{P}\left[\frac{1}{\tau-\tau''}\right]E_\sigma(Q(\tau''))\times G_\sigma(\tau'',\tau')d\tau'' . \tag{34}$$

We can solve for $G_\sigma(\tau,\tau')$ by using the method of Muskhelishivili and by following Sec. III B of Hamann's paper. We find

$$G(\tau,\tau')=-i\frac{N(0)}{4\xi(\tau)}\left[\frac{1}{X^+(\tau)}-\frac{1}{X^-(\tau)}\right]\mathrm{P}\left[\frac{X^+(\tau')+X^-(\tau')-X^+(\tau)-X^-(\tau)}{\tau'-\tau}\right]+\left[\frac{1}{1+\xi^2(\tau)}\right]G^{(0)}(\tau-\tau')-\frac{1}{4}\frac{1}{\xi(\tau)}[X^+(\tau')-X^-(\tau')]\left[\frac{1}{X^+(\tau)}-\frac{1}{X^-(\tau)}\right]D(\tau-\tau') , \tag{35}$$

where

$$\xi(\tau)=g\pi N(0)E(Q(\tau)) , \tag{36}$$

$$X^{\pm}(\tau)=\exp[\pm i\eta(\tau)]\exp\left[\frac{1}{\pi}\mathrm{P}\int_0^\beta\frac{\eta(\tau'')}{\tau''-\tau}d\tau''\right] , \tag{37}$$

$$D(\tau)=\pi N(0)\delta(\tau) , \tag{38}$$

and

$$\eta(\tau)=-\tan^{-1}\xi(\tau) . \tag{39}$$

We have temporarily dropped the σ index. In the $\tau\to 0$ limit, $D(\tau)$ has a spurious divergence of the sort we discussed before. $D(\tau)$ is the asymptotic form of some nonsingular function. If we had not set $\tan\theta=0$, its complete asymptotic form would be

$$D(\tau)=-N(0)\left[\tan\theta\,\mathrm{P}\left[\frac{1}{\tau}\right]-\pi\delta(\tau)\right] , \tag{40}$$

which is similar to the asymptotic form of $G^{(0)}(\tau)$. $\eta(\tau)$ is the "instantaneous phase shift" produced by the dis-

placed atom. Since we do not have a central potential that conserves angular momentum, we cannot use traditional scattering theory to define a phase shift. However, we can consider a constant potential ($V_{\vec{k}\,\vec{k}'}=\lambda Q$) equal to the instantaneous potential. Then, as we show in the Appendix, $\eta(\tau)$ is the phase shift at the Fermi surface produced by this constant potential.[19,21] A constant potential in momentum space is a δ-function potential in real space. Since only s waves have finite amplitude at the origin, $\eta(\tau)$ corresponds to an s-wave phase shift.

In order to evaluate the partition function given in Eq. (26), we require the $\tau'\to\tau^+$ limit of $G(\tau,\tau')$. We can use the exact propagator in Eq. (35) to find $G^{(0)}(\tau=0^-)$:

$$G^{(0)}(\tau=0^-)=\int_{-\infty}^{\infty}N(\epsilon)u(\epsilon)f(\epsilon)d\epsilon=N\ , \tag{41}$$

where N is the number of electrons per atom. We take

$$D(\tau=0^-)=D\ , \tag{42}$$

where $D/N(0)$ is roughly the bandwidth. This is reasonable since the bandwidth sets the energy scale. D is a dimensionless number and must be of order unity. For simplicity we set $D=1$. With these two expressions we can use Eq. (35) for $G_\sigma(\tau,\tau^+)$ to evaluate Z_σ in Eq. (26). The first term in (35) in the "transient" part of G_σ and is identical to Hamann's transient term up to a constant multiplicative factor. It gives rise to the retarded interaction between hops. The last two terms in (35) are the "adiabatic" part of G_σ and they give rise to the effective double-well potential. We have

$$Z=Z_0Z_+Z_-=Z_0\exp\left[-\int_0^\beta d\tau[V(\tau)+T(\tau)]\right]\ , \tag{43}$$

where

$$V(\tau)=\tfrac{1}{2}M\Omega^2Q^2(\tau)-\frac{1}{\pi N(0)}\ln|1+\gamma^2(\tau)|\ , \tag{44}$$

$$T(\tau)=\tfrac{1}{2}M\left[\frac{dQ(\tau)}{d\tau}\right]^2 -\frac{1}{\pi^2}\int_0^\beta d\tau'\ln|\tau-\tau'|\frac{d\gamma(\tau')}{d\tau'} \times\frac{d}{d\tau}\left[\frac{\gamma(\tau)}{\gamma^2(\tau)-\gamma^2(\tau')}\ln\left|\frac{1+\gamma^2(\tau)}{1+\gamma^2(\tau')}\right|\right], \tag{45}$$

and

$$\gamma(\tau)=\pi N(0)E(Q(\tau)) =-\pi N(0)\lambda Q(\tau) =-\left[\frac{\pi}{2}M\Omega^2N(0)\right]^{1/2}\Lambda Q(\tau)\ . \tag{46}$$

For $\gamma(\tau),\gamma(\tau')\ll 1$,

$$T(\tau)\simeq\tfrac{1}{2}M\left[\frac{dQ(\tau)}{d\tau}\right]^2 -\frac{1}{\pi^2}\int_0^\beta d\tau'\ln|\tau-\tau'|\frac{d\gamma(\tau')}{d\tau'}\frac{d\gamma(\tau)}{d\tau}\ . \tag{47}$$

We have included the terms from $H_{\rm ph}$. Notice that $T(\tau)$ and $V(\tau)$ are even functions of $Q(\tau)$. If the coupling Λ is large enough, i.e., if

$$\Lambda>1\ , \tag{48}$$

then $V(\tau)$ will be a symmetric double well (see Fig. 2). Actually, $V(\tau)$ is the sum of the potential due to the "+" electrons and that due to the "−" electrons, i.e., $V(\tau)=V_+(\tau)+V_-(\tau)$, where

$$V_\sigma(\tau)=\tfrac{1}{2}V(\tau)+\frac{N}{\pi N(0)}\tan^{-1}\gamma_\sigma(\tau) \tag{49}$$

and

$$\gamma_\sigma(\tau)=\pi N(0)E_\sigma(Q(\tau))=-\sigma\pi N(0)\lambda Q(\tau)\ . \tag{50}$$

The $\tan^{-1}\gamma$ term is odd in Q and implies that $V(\tau)$ will have more "+" electrons in the right-hand well and more "−" electrons in the left-hand well. This is physically reasonable. If we represent s waves by $\cos Q$ and p waves by $\sin Q$, the "+" electron wave function, which is the symmetric combination of s and p waves, will have greater amplitude for positive Q, and the "−" electron wave function, which is the antisymmetric combination, will have greater amplitude for negative Q. With Eq. (19) we see that a phase shift of 45° ($\gamma=1$) corresponds to

$$q=\frac{2}{\pi N(0)\Omega\Lambda^2}\ .$$

This simply says that one phonon can give a large phase shift if we have a high density of states at the Fermi surface and a large intrinsic phonon stiffness.

The double-well minima $\pm Q_0$ are given by

$$Q_0^2=\frac{1}{\frac{1}{2}M\Omega^2\pi N(0)}\left[1-\frac{1}{\Lambda^2}\right]\ . \tag{51}$$

For strong coupling such that $\Lambda\gg 1$,

$$Q_0^2\simeq\frac{1}{\frac{1}{2}M\Omega^2\pi N(0)}\ , \tag{52}$$

which is independent of Λ. This differs from the Jahn-Teller result (18), because there we neglected the band electrons. The formation of a double well implies that the atom prefers to be displaced from its lattice site if the coupling is sufficiently strong. When the atom moves to the right or the left, the positive charge of it and its neighbor attracts an electron cloud, which, in turn, makes the

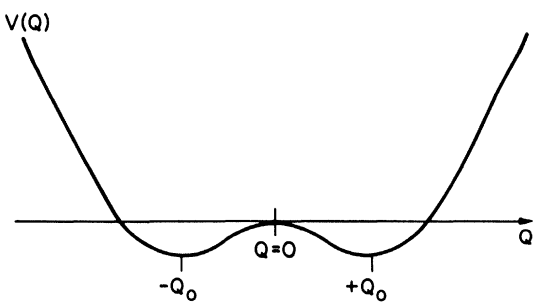

FIG. 2. Symmetric double-well potential.

environment seen by the atom more favorable. Q_0 is the place where the repulsion of the neighboring atom is exactly compensated for by the attraction of the electron cloud. If this attraction is sufficiently strong, i.e., if Λ is large enough, $Q_0 \neq 0$. This idea is similar to that of a negative-U potential. Notice that the well cannot be infinitely deep; the ion can capture at most one or two electrons. If there were no dynamics, i.e., if $T(\tau)=0$, then a charge-density wave would form and the atoms would dimerize along the chains in the $A15$ compounds. For the Anderson model (AM) form of the local-phonon Hamiltonian given in Eqs. (10a), (13), and (14), the effective potential is

$$V_\sigma^{\mathrm{AM}}(\tau)=\tfrac{1}{4}M\Omega^2Q^2(\tau)+\tfrac{1}{2}\Delta\xi_0(\tau) -(\Delta/\pi)[\xi_\sigma(\tau)\tan^{-1}\xi_\sigma(\tau)-\tfrac{1}{2}\ln|1+\xi_\sigma^2(\tau)|], \tag{53}$$

where

$$\xi_\sigma(\tau)=\frac{E_\sigma(Q(\tau))}{\Delta}=-\sigma\left[\frac{\pi M\Omega^2}{2\Delta}\right]^{1/2}\Lambda Q , \tag{54}$$

and $\Delta=\pi N(0)|V_{\vec{k}0}|^2$ is the resonance width and is of the order of the bandwidth. $T^{\mathrm{AM}}(\tau)$ is identical to $T(\tau)$ given in Eq. (45) if $\gamma(\tau)$ is replaced by

$$\xi(\tau)=\frac{E(Q(\tau))}{\Delta}=-\left[\frac{\pi M\Omega^2}{2\Delta}\right]^{1/2}\Lambda Q . \tag{55}$$

By comparing the expressions for $V(\tau)$ given by Eqs. (44) and (53), we can identify $1/N(0)$ with Δ from the coefficient of the logarithmic term. Although, for small ξ and γ, these equations are the same, their general functional forms are slightly different. In deriving the effective potential, we used the zero-time limit of the exact free propagator. For the free-band model this is given in Eq. (32). For the Anderson model it is[17]

$$G^{(0)}(\tau=0^-)=\frac{1}{2}-\frac{1}{\pi}\tan^{-1}\left[\frac{E_0}{\Delta}\right] .$$

Thus the effective potentials are different because the ultraviolet properties of the models are different as is reflected in $G^{(0)}(\tau=0^-)$. However, the infrared properties are the same.

The second term in $T(\tau)$ given by Eq. (45) is not local in time and describes the retarded interactions between hops from one well to the other. There is a retarded interaction because the Fermi gas provides a "memory" for the motions of the atom. When the atom hops, it produces density waves in the electron gas, which, in turn, affect the next hop. This is where we see the breakdown of the adiabatic approximation: If the electrons were always in equilibrium with the phonon, there would be no retarded interactions. This is an important difference between the local-phonon model and the dynamic Jahn-Teller effect which assumes that the adiabatic approximation is valid.[22]

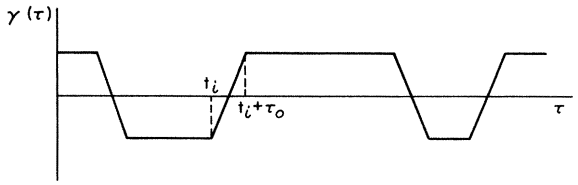

FIG. 3. Typical hopping path.

The complete partition function Z is found by integrating the partition function $Z(\gamma)$ for a particular path over all paths,

$$Z=Z_0\int\delta\gamma\, Z(\gamma) .$$

Since the paths are weighted by a Boltzmann factor, the dominant path is the one in which the atom just sits in one well. Hopping paths such as the one in Fig. 3 are less likely to occur because they cost kinetic energy, but their lessened probability is more than compensated for by the large number of them, and they make an important contribution to the partition function. In order to evaluate the $d\tau$ integral in Eq. (43), we will consider linear hopping paths with $\gamma(0)=\gamma(\beta)=0$,

$$\gamma(\tau)=-\gamma_0+\frac{2\gamma_0}{\tau_0}(\tau-t_i) , \tag{56}$$

which describes a hop from $-\gamma_0$ to $+\gamma_0$ where

$$\gamma_0=-[\pi N(0)\tfrac{1}{2}M\Omega^2]^{1/2}\Lambda Q_0=-(\Lambda^2-1)^{1/2} . \tag{57}$$

Notice that γ_0 is determined solely by the coupling. The hop takes place during an interval τ_0. These paths are a mathematical convenience. It would be more accurate to use instantons or hops that obey the classical equations of motion, but this would not change the essential physics. We are also ignoring fluctuations about the minimum of each well and within each hop. This is consistent with the Nozières—De Dominicis approximation which is valid at long time scales. We expect high-frequency fluctuations to be important only at short time scales.

Between hops, when the atom is sitting in a well, the contribution to the potential energy is

$$-\int_{0\ (\text{without the hops})}^{\beta}d\tau\, V(\tau)=-(\beta-2n\tau_0)\left[\tfrac{1}{2}M\Omega^2Q_0^2-\frac{1}{\pi N(0)}\ln|1+\gamma_0^2|\right] \tag{58}$$

for a path with $2n$ hops. During a hop, the potential energy gives

$$-\int_{t_i}^{t_i+\tau_0}d\tau\, V(\tau)=-\tau_0\left[\tfrac{1}{6}M\Omega^2Q_0^2-\frac{1}{\pi N(0)}\left[\ln|1+\gamma_0^2|-2+\frac{2}{\gamma_0}\tan^{-1}\gamma_0\right]\right] . \tag{59}$$

Our evaluation of $\int d\tau\, T(\tau)$ is identical to that used by Hamann in Sec. IV B of his paper. We consider paths such that

the derivative of $\gamma(\tau)$ is zero unless $t_i<\tau<t_i+\tau_0$. Then $T(\tau)$ is nonzero only when both τ and τ' are inside hops. Up to small additive constants,

$$-\int_0^\beta T(\tau)d\tau=-\frac{4nMQ_0^2}{\tau_0}-\sum_{i=1}^{2n}\ln|\gamma_0|+2\left[\frac{2\tan^{-1}\gamma_0}{\pi}\right]^2\sum_{\substack{i,j\\ i>j}}\left[(-1)^{i-j}\ln\left|\frac{2(t_i-t_j)}{\tau_0}\right|\right], \tag{60}$$

where we have assumed that γ_0 is large such that $\ln|\gamma_0|\gg 4/\pi|\gamma_0|$. The first term in (60) comes from integrating the kinetic energy term $\frac{1}{2}M\dot{Q}^2$. To obtain the full partition function we must sum over all possible even numbers of hops and integrated over the position of each hop. Two hops cannot be closer to each other than τ_0. Our result is

$$Z=Z_0\sum_{n=0}^{\infty}\exp[-\beta V(Q_0)]y^{2n}\int_0^\beta\frac{dt_{2n}}{\tau_0}\int_0^{t_{2n}-\tau_0}\frac{dt_{2n-1}}{\tau_0}\cdots\int_0^{t_2-\tau_0}\frac{dt_1}{\tau_0}\exp\left[\alpha\sum_{i>j}(-1)^{i-j}\ln\left|\frac{t_i-t_j}{\tau_0}\right|\right], \tag{61}$$

where $V(Q)$ is given by Eq. (44). We write

$$\alpha=2\left[\frac{\tan^{-1}\gamma_0}{\pi/2}\right]^2=2\left[\frac{\eta_0}{\pi/2}\right]^2, \tag{62}$$

where η_0 is the scattering phase shift associated with the displacement Q_0. The hopping fugacity is given by

$$y=\frac{1}{\gamma_0}2^{-\alpha/2}e^{-2MQ_0^2/\tau_0}\exp\left\{-\tau_0\left[\tfrac{1}{3}M\Omega^2Q_0^2-\frac{1}{\pi N(0)}\left[2-\frac{2}{\gamma_0}\tan^{-1}\gamma_0\right]\right]\right\}. \tag{63}$$

This contains contributions from the potential energy, from $\frac{1}{2}MQ^2$, and from the retarded interaction of a hop with itself. Physically, the fugacity is the tendency or probability for a hop to occur on a given time scale. We can determine τ_0 by varying it to minimize the energy of a path. The contribution to the energy that depends on τ_0 is

$$E(\tau_0)=-2n\tau_0A(Q_0)+\frac{4nMQ_0^2}{\tau_0}-2n\left[\frac{\alpha}{2}\right]\ln\tau_0, \tag{64}$$

where

$$A(Q_0)=\tfrac{1}{3}M\Omega^2Q_0^2-\frac{1}{\pi N(0)}\left[2-\frac{2}{\gamma_0}\tan^{-1}\gamma_0\right]. \tag{65}$$

Minimizing $E(\tau_0)$, we obtain

$$\tau_0=-\frac{\alpha}{2}+\left[\left[\frac{\alpha}{2}\right]^2-\frac{8AMQ_0^2}{\hbar^2}\right]^{1/2}\Big/(2A/\hbar). \tag{66}$$

(We have inserted $\hbar$ to make it easier to do numerical estimates later.) Knowing that τ_0 minimizes the hopping energy allows us to rewrite the fugacity as

$$y=(1/\gamma_0)(2e)^{-\alpha/2}e^{-m}, \tag{67}$$

where the dimensionless measure of the mass is

$$m=4MQ_0^2/\tau_0.$$

Notice that y no longer depends explicitly on the potential. The small additive constants [see Eq. (125)] which we neglected in Eq. (60) will affect y only by a factor of order unity.

V. SCALING

The form of the partition function given in Eq. (61) is the same as that found by Yuval and Anderson for the Kondo problem.[16] Comparing our expression and theirs, we can identify

$$y\leftrightarrow J_\perp\tau/2,\quad \alpha\leftrightarrow 2-\epsilon. \tag{68}$$

There is a logarithmic interaction between flips or hops such that neighboring flips attract with an interaction strength α. Since $\alpha\le 2$ corresponds to $\epsilon>0$ in Eq. (68), the local-phonon system maps onto the antiferromagnetic Kondo problem. We can see this more clearly by applying the space-time scaling technique of Anderson, Yuval, and Hamann.[18] The resulting scaling relations are

$$d\alpha=-4\alpha y^2d(\ln\tau), \tag{69}$$

$$dy=\tfrac{1}{2}y(2-\alpha)d(\ln\tau). \tag{70}$$

These were derived assuming a small fugacity, $y\ll 1$, i.e., assuming a rare gas of flips. In general, the average spacing between flips is much greater than τ, i.e., $\tau\ll|t_i-t_j|$. As in the Kondo problem, we have ignored the explicit τ_0 dependence of y. If we had not done so, we would have found

$$dy=y[\tfrac{1}{2}(2-\alpha)-m(\tau_0)]d(\ln\tau_0).$$

We shall see that (69) and (70) imply that the second term is irrelevant, i.e., $m(\tau_0)$ scales to zero.

In the region of $y\ll 1$ and $\alpha\simeq 2$, the scaling equations become

$$\frac{d\epsilon}{dl}=8y^2, \tag{71a}$$

$$\frac{dy}{dl}=\tfrac{1}{2}y\epsilon, \tag{71b}$$

where

$$l=\ln\tau, \tag{72}$$

$$\epsilon=2-\alpha, \tag{73}$$

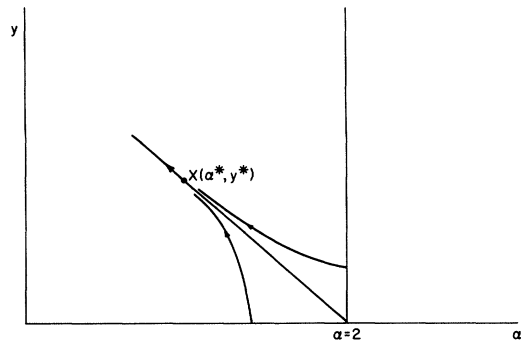

FIG. 4. Scaling diagram.

and τ is measured in units of the Kondo time τ_K which is a characteristic time scale. τ_K is the average length of the section of the path dominated by one minimum. Dividing (71a) by (71b) and integrating yields hyperbolic scaling curves,

$$\epsilon^2-16y^2=\text{const} . \tag{74}$$

These curves are shown in Fig. 4. They indicate that the system scales from small to large fugacity and from a large phase shift to a small phase shift, i.e., from large to small electron-phonon coupling. It makes sense physically to have large Λ associated with low fugacity because it brings to mind a picture of the atom tied down in one of the minima of a deep double well by the electrons. To understand how the coupling is related to the phase shift and the fugacity, we return to Eqs. (57), (62), and (67). As η_0 is renormalized downward, so is $|\gamma_0|$ and hence Λ. From (67) we see that y grows roughly as $1/\gamma_0$. This increase in the fugacity can be interpreted as an increase in the hopping probability or as a more transparent barrier. The depth of the double well is determined by $\ln|1+\gamma_0^2|$ according to Eq. (44). Thus the well becomes shallower as γ_0 decreases.

The renormalization-group procedure consists of increasing τ_0, or equivalently, of decreasing bandwidth. This is related to lowering the temperature of the system, because the dimensionless quantity which scales is β/τ_0. To see this, let $t'=t/\tau_0$ in Eq. (60),

$$Z=Z_0\sum_{n=0}^{\infty}e^{-\beta V(Q_0)}y^{2n}\int_0^{\beta/\tau_0}dt'_{2n}\int_0^{t'_{2n}-1}dt'_{2n-1}\cdots\int_0^{t'_2-1}dt'_1\exp\left[\alpha\sum_{\substack{i,j\\ i>j}}(-1)^{i-j}\ln|t'_1-t'_j|\right] . \tag{75}$$

Setting the ground-state energy $V(Q_0)=0$, we see that β enters Z only in the combination β/τ_0. Lowering the temperature of the system ($\beta-\Delta\beta\rightarrow\beta$) will change the parameters τ, α, and y in a way prescribed by the scaling relations. More explicitly,

$$\begin{aligned}Z((\beta-\Delta\beta)/(\tau-\Delta\tau),y,\alpha)&=Z((\beta/\tau),y,\alpha)\\&=e^{\beta\Delta F}Z((\beta/\tilde{\tau}),\tilde{y},\tilde{\alpha}) ,\end{aligned} \tag{76}$$

where $\beta\Delta F=(\beta/\tau)y^2d(ln\tau)$ gives the shift in the ground-state energy $V(Q_0)$. $\tilde{\tau}$, $\tilde{y}$, and $\tilde{\alpha}$ are the renormalized parameters. Notice that β contributes to this shift only in the ratio β/τ_0. Thus longer time scales correspond to lower temperatures.

We must stop scaling when $\tau=\beta$. The lower the temperature is, the farther we can go along a scaling trajectory. When $\beta/\tau=1$, then $l=d(\ln\tilde{\tau})=d(\ln\beta)$, and $\alpha(l)$ and $y(l)$ will depend on the cutoff $\tilde{\tau}$ in the same way that they depend on the inverse temperature β. Suppose our system initially has $\alpha_0\sim2$ and $y_0\ll1$. At high temperatures we are still close to our starting point, the fugacity is still low, and the average path is ordered in the sense that the atom is predominantly in one minimum or the other. At low temperatures we have scaled to large fugacity; the paths are disordered and the atom tends to flip back and forth between the wells rather than sit still. This is the analog of the Kondo singlet.

We should remark that our basic approximation to replace optical phonons with Einstein oscillators is applicable only at high temperatures $T\gtrsim T_D$, where $T_D\sim40$ K is the temperature associated with the width of the optical-phonon dispersion curve.[23] The flat dispersion curve of these independent oscillators means that these phonons are localized with zero group velocity and infinite effective mass. The idea that each atom is "unaware" of its neighbors and "sees" only the surrounding electron gas is consistent with having a large electron-phonon coupling and a large amount of screening at high temperatures. As we lower the temperature and crossover into the region of the scaling diagram dominated by the weak-coupling fixed point, the atom begins to interact with its neighbors and to transfer energy to them, i.e., the local phonon is able to hop to neighboring sites. Thus we obtain acoustic phonons.

However, our calculation of the partition function involved a zero-temperature approximation in which we replaced the Fermi function by a step function. How will our results be affected by the fact that the local-phonon model is only valid at high temperatures where thermal fluctuations dominate the physics? In dealing with path integrals, we only considered quantum tunneling between the minima of the double well. This is valid as long as the time between the ith and jth hops satisfies the inequality

$$\tau_0\ll t_i-t_j\ll\beta . \tag{77}$$

The condition $\tau_0\ll t_i-t_j$ implies that there is a rare gas of flips. This assumption was used in deriving the scaling relations. The other half of (77), $t_i-t_j\ll\beta$, describes the region in which Eq. (61) is a valid approximation for the partition function. A finite-temperature calculation of Z with linear hops would result in the replacement

$$\ln\left|\frac{t_i-t_j}{\tau_0}\right|\rightarrow\ln\left|\frac{\beta}{\pi\tau_0}\sin\left[\frac{\pi(t_i-t_j)}{\beta}\right]\right| , \tag{78}$$

for $\tau_0\ll|t_i-t_j|<\beta$. In the spirit of "poor-man's scaling," we can restate (77) in terms of a band picture.[24] The

idea is simply to reduce the band cutoff E_c down to k_BT. Quantum fluctuations dominate between E_c and k_BT so we can eliminate these in our scaling procedure. (We set $\epsilon_F=0$.) We stop scaling at k_BT. Below k_BT thermal fluctuations dominate.

We have also ignored thermal (and quantum) fluctuations about the minimum of each well. This will increase the hopping fugacity, especially at high temperatures. This can be quite important if the barrier height is low which, as we shall see, seems to be the case in real systems [$V(Q_0)\sim$ a few meV]. The basic conclusion is that our low-temperature calculation of our high-temperature model is correct in terms of the basic physics, although a finite-temperature calculation would change some numerical factors.

The characteristic temperature below which quantum fluctuations become large in our problem is given by the Kondo temperature T_K. To find T_K we follow Young and Bohr.[25] In the neighborhood of $\alpha=2$ and $y\ll 1$, the scaling equations are (71a) and (71b). The asymptote or separatrix of the scaling hyperbolas is given by

$$\epsilon=4y\ . \tag{79}$$

Above the separatrix the solution of Eq. (71) is

$$\epsilon(l)=a\cot\left[\phi-\frac{a}{2}l\right], \tag{80a}$$

$$y(l)=\tfrac{1}{4}a\csc\left[\phi-\frac{a}{2}l\right], \tag{80b}$$

with

$$\cos\phi=\epsilon_0/4y_0,\quad 0\le\phi\le\pi \tag{80c}$$

and

$$\epsilon^2-16y^2=-a^2,\quad a>0 \text{ and real}\ . \tag{80d}$$

Similarly the solution below the separatrix is

$$\epsilon(l)=a'\coth\left[\theta-\frac{a'}{2}l\right], \tag{81a}$$

$$y(l)=\tfrac{1}{4}a'\operatorname{csch}\left[\theta-\frac{a'}{2}l\right], \tag{81b}$$

with

$$\cosh\theta=\epsilon_0/4y_0 \tag{81c}$$

and

$$\epsilon^2-16y^2=a'^2,\quad a'>0 \text{ and real}\ . \tag{81d}$$

Note that all trajectories starting near the point $(\epsilon=0,y=0)$ pass arbitrarily close to some point X on the separatrix where the fugacity is y^*. y^* is still sufficiently small for the scaling relations to be valid. The characteristic length scale $\xi=\tau_K$ in this region can be found by relating it to the value ξ would have for a model with ϵ^* and y^*. Since ξ scales as[26]

$$\xi=e^l\xi(l)\ ,$$

we can determine τ_K by setting $l=l^*$. Following Young and Bohr,[26] we obtain

$$\tau_K=Ae^{l_0}\ ,$$

where

$$l_0=\frac{\phi}{2y_0\sin\phi} \tag{82a}$$

above the separatrix, and

$$l_0=\frac{\theta}{2y_0\sinh\theta} \tag{82b}$$

below the separatrix. l_0 is the point where $\epsilon(l)$ and $y(l)$ diverge. A is the overall scale factor on the order of τ_0. τ_K gives the crossover time scale from strong coupling to weak coupling.

Another way to define this crossover is to ask for the temperature T_A below which quantum tunneling through the double-well barrier dominates and above which thermal activation over the barrier dominates. Affleck has treated this problem for a one-particle metastable state (Fig. 5).[27] He considered the competition between the tendency for the lower-energy levels to be populated according to the Boltzmann distribution and the tendency for the majority of the tunneling particles to come from the higher levels. He showed that the quantum tunneling rate is equal to the rate of thermal fluctuations at a temperature $T_A=\hbar\omega/2\pi k_B$, where $-M\omega^2$ is the curvature at the top of the barrier,

$$-M\omega^2=\left.\frac{d^2V}{dQ_2}\right|_{Q=0}=M\Omega^2(1-\Lambda^2)\ .$$

Although decay rates are ill defined for a symmetric double well, T_A can still give a useful estimate of the crossover. However, we should keep in mind that the coupling Λ, and, hence, the double well itself, are renormalized as the temperature decreases.

We now insert a few numbers and make some crude estimates. We will consider V_3Si as a typical example. In the cubic phase the lattice constant is 4.72 Å. The mass of a vanadium atom is 51 amu or 5×10^{-27} eV sec^2/Å^2. As we mentioned before, the specific-heat data implies that the total density of states at the Fermi surface is approximately 2.4 states/eV atom.[6] For one type of electron we take $N(0)\sim1.2$ states/eV atom. We can estimate a

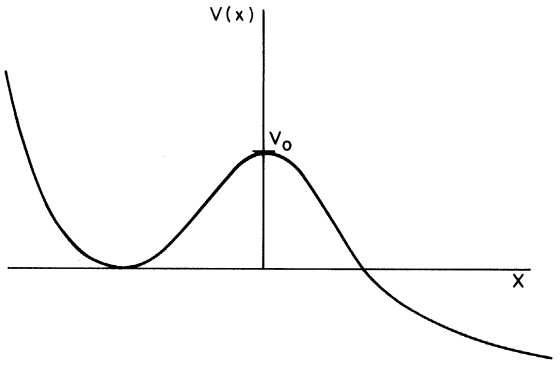

FIG. 5. Potential for a one-dimensional metastable system.

typical atomic excursion due to thermal vibrations by saying that $k_B\Theta_D$ is roughly equal to $\frac{1}{2}M\omega^2x^2$. Taking the Debye temperature Θ_D to be 300 K and the phonon frequency ω to be 2π (4×10^{12} sec^{-1}), we obtain $x\sim0.1$ Å. Note that this is much larger than a displacement due to the martensitic transition which is only a few thousandths of an angstrom. Above several hundred degrees Kelvin, the elastic stiffness of the $A15$ compounds is normal.[8] This means that the mean thermal amplitude of the atom's vibrations is such that the atom spends most of its time on the walls of the potential well. The bare or intrinsic stiffness, however, will be quite a bit larger than the renormalized stiffness which is observed. In the $A15$ compounds the distance between vanadium atoms along a chain is 10% less than in pure vanadium. This implies that the intrinsic stiffness must be large. This stiffness is softened by the strong electron-phonon interaction. As we have seen in the case of Tomonoga bosons, the large coupling Λ which is needed to account for the large resistivity must be accompanied by a sizable stiffness to prevent the phonons from becoming soft. We have shown elsewhere[28] that the ratio $\Omega^2_{\text{intrinsic}}/\Omega^2_{\text{observed}}$ will be comparable to the ratio $\Lambda(A15)/\Lambda$(normal metal). To estimate the intrinsic stiffness $\frac{1}{2}M\Omega^2$, we note that 50 meV is a typical optical-phonon energy. We will set the bare energy to be 100 times larger, namely $\frac{1}{2}M\Omega^2Q^2=4$ eV. $Q\sim0.1$ Å implies

$$\tfrac{1}{2}M\Omega^2=400\ \text{eV/Å}^2\ .$$

Let us consider the condition

$$\Lambda=2\ .$$

Equation (51) gives $Q_0\sim0.02$ Å which roughly corresponds to 1.5 phonons, according to Eq. (19). Equation (44) gives a well depth of

$$V(Q_0)\sim-170\ \text{meV}\ .$$

Notice that this is much too shallow for us to be concerned with Hubbard U effects since $U\sim10$ eV. It is also too shallow to localize electrons which have energies on the order of $\epsilon_F\sim1$—10 eV. Thus it is unlikely that phonons localize electrons. It is useful to compare the barrier height $-V(Q_0)$ with the zero-point energy $\frac{1}{2}\hbar\omega_b$ about each minimum, where the curvature at the bottom is given by

$$M\omega_0^2=\left.\frac{d^2V}{dQ^2}\right|_{Q=Q_0}=M\Omega^2\left[1-\frac{\Lambda^2}{1+\gamma_0^2}\left[1-\frac{2\gamma_0^2}{1+\gamma_0^2}\right]\right]\ . \tag{83}$$

In this case,

$$\tfrac{1}{2}\hbar\omega_b\sim160\ \text{meV}\ ,$$

which is comparable to $V(Q_0)$ and indicates that fluctuations within each well are an important contribution to the rate of hopping. From Eq. (66) the hopping time is

$$\tau_0\sim1\times10^{-14}\ \text{sec}\ ,$$

which corresponds to a temperature

$$T_0\sim\pi\hbar/k_B\tau_0\sim2400\ \text{K}$$

if τ_0 is roughly half a period ($\omega_0=\pi/\tau_0$). α, which is related to the phase shift, is given by Eq. (62),

$$\alpha=0.89\ ,$$

which implies that the phase shift $\delta\sim60°$. The fugacity and the dimensionless mass given by Eq. (67) are

$$y\sim0.06,\quad m\sim1.5\ .$$

Setting $A=\tau_0$ in Eq. (82a), we find that the Kondo time

$$\tau_K\sim5.6\times10^{-13}\ \text{sec}\ ,$$

which corresponds to a Kondo temperature of

$$T_K\sim2\pi\frac{\hbar}{k_B\tau_K}\sim86\ \text{K}\ .$$

This is in the correct temperature range as far as the $A15$'s are concerned. In the vicinity of T_K we expect to see the crossover from strong coupling to weak coupling. Above T_K one should apply perturbation theory about the $\Lambda=\infty$ fixed point which corresponds to $\alpha=2$ and $y=0$ according to Eqs. (46) and (62). T_K decreases as Λ increases because the larger Λ is initially, the farther we must go along the scaling trajectory to obtain the crossover. Suppose we increase the coupling such that $\Lambda=10$. This increases the barrier height [$V(Q_0)\sim-960$ meV] and decreases the tunneling rate which depends exponentially on $[MV(Q_0)]^{1/2}$. Thus the fugacity drops to

TABLE I. Sample values. $M_V=5\times10^{-27}$ eV sec^2/Å^2 is the mass of the vanadium atom.

Λ	$\frac{1}{2}M\Omega^2$ $\left[\frac{\text{eV}}{\text{Å}^2}\right]$	$N(0)$ $\left[\frac{\text{states}}{\text{eV atoms}}\right]$	Q_0 (Å)	$V(Q_0)$ (meV)	$\frac{1}{2}\hbar\omega_0$ (meV)	Phase shift η (deg)	α	y	l_0	$T_0=\frac{\pi\hbar}{k_B\tau_0}$ (K)	$T_K=\frac{2\pi\hbar}{k_B\tau_k}$ (K)
1.5	400	1.2	0.019	−68	140	48	0.57	0.25	1.8	1700	590
2	400	1.2	0.022	−170	160	60	0.89	6×10^{-2}	4.0	2400	86
2	400	0.5	0.035	−410	160	60	0.89	5×10^{-3}	8.6	2700	1
5	400	1.2	0.025	−600	180	78	1.5	3×10^{-3}	18	3500	1×10^{-4}
10	400	1.2	0.026	−960	190	84	1.8	9×10^{-4}	40	4000	3×10^{-14}
1.5	100	1.2	0.038	−68	70	48	0.57	0.09	3.0	1000	99
1.5	4	1.2	0.19	−68	14	48	0.57	2×10^{-5}	7.0	220	2×10^{-4}

$\sim 9\times 10^{-4}$. The Kondo temperature, which in turn depends exponentially on y, decreases dramatically to 3×10^{-14} K. Thus T_K is very sensitive to Λ. We also note the phase shift $\delta\sim 84°$, which corresponds to $\alpha\sim 1.8$. We can estimate $T_A=\hbar\omega/2\pi k_B$, which is the crossover temperature between thermal and quantum fluctuations. Using the same set of parameters as above with $\Lambda=2$, we find $T_A\sim 850$ K. The order of magnitude of T_A is largely determined by the intrinsic stiffness of the well. Sample values are listed in Table I for convenience. The input parameters are Λ, $\frac{1}{2}M\Omega^2$, and $N(0)$. According to Eq. (57), the phase shift, and hence α, are determined solely by Λ and are not affected by the stiffness or the density of states. Increasing the stiffness causes y, T_0, and T_K to increase and Q_0 to decrease. Decreasing the density of states results in an increase in Q_0 and T_0 and a decrease in y and T_K.

VI. SPECIFIC HEAT AND SUSCEPTIBILITY

We now turn to a rough comparison of our model with experimental data. The parameters in the Hamiltonian, and thus α and y, depend on time scale and temperature. The initial parameters include fluctuations on time scales shorter than τ_0 which is the shortest time scale in the problem. Once we have renormalized α and y to include all fluctuations on time scales shorter than β, we have the temperature-dependent quantities $\alpha(\beta)$ and $y(\beta)$. To calculate the specific heat, we first scale the partition function until $l=\ln\beta$,

$$Z=\exp\left[\int_{\tau_0}^{\beta} y^2\frac{\beta}{\tau}d(\ln\tau)\right]\tilde{Z}\ , \tag{84}$$

where the exponential factor is the shift in the ground-state energy which we noted in Eq. (76) and where

$$\tilde{Z}=Z((\beta/\tilde{\tau})=1,\tilde{y},\tilde{\alpha})\ .$$

If the fugacity is low, we can expand the partition function in Eq. (61) to lowest order in $y\ll 1$,

$$\tilde{Z}\simeq Z_0 e^{-\beta V(Q_0)}\left\{1+\frac{\tilde{y}^2}{1-\tilde{\alpha}}\left[\frac{1}{2-\tilde{\alpha}}\left[\frac{\beta}{\tilde{\tau}}\right]^{2-\tilde{\alpha}}-\frac{\beta}{\tilde{\tau}}\right]\right\}\Bigg|_{\beta=\tilde{\tau}}$$

$$\simeq Z_0 e^{-\beta V(Q_0)}\left[1+\frac{\tilde{y}^2}{1-\tilde{\alpha}}\left[\frac{1}{2-\tilde{\alpha}}-1\right]\right]\ . \tag{85}$$

The corresponding "high-temperature" specific heat is given by

$$C=k_B\beta^2\frac{\partial^2\ln Z}{\partial\beta^2}\ . \tag{86}$$

Near $\alpha\simeq 2, y\ll 1$, we can expand our expressions (80) and (81) for $\epsilon(l)$ and $y(l)$ to lowest order in l/l_0, where $l_0=2\phi/a$ is the point at which $\epsilon(l)$ and $y(l)$ diverge. We assume that $\phi-(a/2)l\ll 1$ which implies that the scaling trajectory is near the separatrix, i.e., $\epsilon(l)\simeq 4y(l)$. We can also assume that a is small such that $a\ll\phi-(a/2)l$. This means that y is small and that the scaling relations are still valid. Then for $(l/l_0)\ll 1$ and $l=\ln\beta$,

$$C=C_{\rm el}+\frac{2k_B}{l_0^2}\left[\frac{1}{8}+\frac{2}{l_0^3}+\frac{2}{l_0^4}\right]$$

$$-\frac{2k_B}{l_0^3}\left[\frac{1}{4}-\frac{3}{2l_0}+\frac{10}{l_0^3}+\frac{12}{l_0^4}\right]\ln\left|\frac{T}{T_K}\right|\ , \tag{87}$$

where $C_{\rm el}$ is the specific heat due to a free gas of electrons with two spin components. The terms which depend on l_0 are a negligible correction to C. Using

$$l_0=\frac{2\theta}{a}=\frac{1}{2y_0}\frac{\theta}{\sinh\theta}\ , \tag{88}$$

we see from Table I that $\Lambda=10$ corresponds to $\alpha_0=1.8$ and $l_0=40$. As a result, the l_0 terms are a negligible contribution to the specific heat. We can use the specific heat to define $\gamma(T)$ and an effective density of states for one spin species and both types of electrons as

$$\gamma(T)=\frac{C}{T}=\frac{2\pi^2}{3}k_B^2 N_{\rm eff}(0)\ . \tag{89}$$

This will give us a temperature-dependent density of states. Even though $\gamma(T)$ comes from the specific heat for the entire system consisting of electrons plus a local phonon, most of the contribution to the specific heat comes from the electrons. Thus, $N_{\rm eff}(0)$ really is an electron density of states.

The Pauli susceptibility is proportional to the density of states and therefore will be temperature dependent in the case of the local phonon,

$$\chi_{\rm Pauli}=2\mu_B^2 N_{\rm eff}(0)\ , \tag{90}$$

where the factor of 2 is for two spins states and μ_B is the Bohr magneton. In the region $\alpha\simeq 2$ and $y\ll 1$, we have

$$\chi_{\rm Pauli}=2\mu_B^2 N(0)+\frac{6\mu_B^2}{\pi^2 k_B l_0^2}\left[\frac{1}{8}+\frac{2}{l_0^3}+\frac{2}{l_0^4}\right]\frac{1}{T}$$

$$-\frac{6\mu_B^2}{\pi^2 k_B l_0^3}\left[\frac{1}{4}-\frac{3}{2l_0}+\frac{10}{l_0^3}+\frac{12}{l_0^4}\right]\frac{\ln|T/T_K|}{T}\ . \tag{91}$$

Once again, the large value of l_0 means that the Pauli susceptibility will have negligible temperature dependence.

We can solve the scaling relations in the vicinity of $\alpha=1, y\ll 1$ and again determine the temperature dependence of the susceptibility and the specific heat. In this neighborhood the scaling equations become

$$\frac{d\alpha}{dl}\simeq -4y^2\ , \tag{92a}$$

$$\frac{dy}{dl}\simeq\tfrac{1}{2}y\ . \tag{92b}$$

The scaling trajectories are parabolas satisfying the relation

$$\alpha^2+4y^2=b\ , \tag{93}$$

where b is a constant. Denoting the initial values of l, α, and y by $l_c=\ln\tau_0$, α_0, and y_0, we can express the solution of (92) as

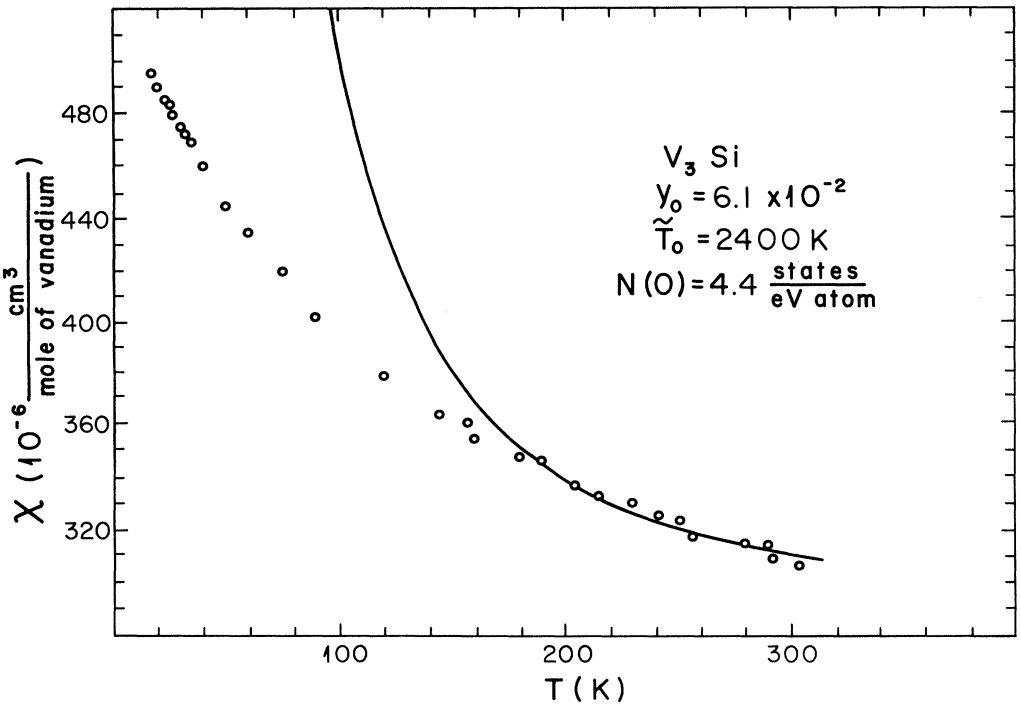

FIG. 6. Fit to the V_3Si susceptibility data of Maita and Bucher (Ref. 31).

$$y(l)=y_0 e^{(l-l_c)/2},\quad y(\tau)=y_0\left[\frac{\tau}{\tau_0}\right]^{1/2}, \tag{94a}$$

$$\alpha(l)=\alpha_0+4y_0^2-4y_0^2 e^{(l-l_c)},\quad \alpha(\tau)=1+4y_0^2\left[1-\frac{\tau}{\tau_0}\right]. \tag{94b}$$

Taking $\tau=\beta$ and using Eqs. (84)—(86), (89), (90), and (94), we find, to order y_0^2,

$$C=C_{\rm el}+\frac{2k_B y_0^2\tilde{T}_0}{T}+\frac{4k_B y_0^2\tilde{T}_0^2}{(T-\tilde{T}_0)^2}, \tag{95}$$

$$\chi_{\rm Pauli}=2\mu_B^2 N(0)+\frac{6\mu_B^2 y_0^2\tilde{T}_0}{\pi^2 k_B T^2}+\frac{12\mu_B^2 y_0^2\tilde{T}_0^2}{\pi^2 k_B T(T-\tilde{T}_0)^2}, \tag{96}$$

where

$$\tilde{T}_0=\hbar/k_B\tau_0 .$$

This differs by a factor of π from our previous definition of T_0 in Table I. Notice that the specific heat and the susceptibility diverge at $T=\tilde{T}_0$. This is a spurious divergence which is symptomatic of the breakdown of the Nozières—De Dominicis approximation near the cutoff. Equation (77) implies that our calculation is only valid for $T\ll T_0$.

Although specific-heat measurements have been made on $A15$ compounds up to 400 K, we make no attempt to compare our results with experiment because of the difficulty in separating the lattice and electronic contributions to the specific heat.[29,30] In addition, the anharmonic localized oscillators constitute only a few of the 10—20 degrees of freedom in the unit cell. However, we do show a fit in Fig. 6 to the high-temperature susceptibility data for V_3Si.[31] The solid line is given by Eq. (96) with $N(0)=4.7$ states/eV atom, $\tilde{T}_0=2400$ K, and $y_6=6.1\times10^{-2}$. Considering the crudeness of our approximations, the fit looks reasonable in the high-temperature region ($T>200$ K) where we expect our model to be valid and where the fugacity is small. A similar fit can be made to the Nb_3Sn data of Rehwald *et al.*[32] Notice that if y_0 is very small in Eqs. (95) and (96), then the specific heat and susceptibility will only be weakly temperature dependent. From Table I we see that small values of y_0 result from small values of $N(0)$ and $\frac{1}{2}M\Omega^2$. The coupling strength is such that $\alpha\simeq1$. Thus the small susceptibility of Nb_3Sb and its weak temperature dependence are consistent with a low density of states.[33] However, we shall see later that this material is quite stiff.

We can view the χ-versus-T curves as $N_{\rm eff}(0)$-versus-T curves, i.e., they show how the density of states depends on temperature. The physical reason why the susceptibility increases with decreasing temperature is quite simple. Suppose that at high temperatures the coupling is large, the double well is deep, and the fugacity is low. The electrons which make the well deep must pair their spins in order to increase their density in the vicinity of the minima. These are resonant, not bound, states. As the well becomes shallower with decreasing temperature, the local electron density decreases and hence, fewer electrons are paired. Thus it is easier for an external magnetic field to polarize the spins, i.e., the susceptibility increases as the temperature decreases. A magnetic field stabilizes the lattice because it inhibits the ability of the electrons to pair. Thus the double well is shallower and the lattice is more stable. This stabilization is seen experimentally.[31]

Clogston and Jaccarino[7,34] showed that the Knight shift

has the same temperature dependence as the Pauli susceptibility up to a minus sign,

$$K_V(T)=K_s-B\chi_{\text{Pauli}}(T)\ , \tag{97}$$

where $K_V(T)$ is the Knight shift of vanadium, K_s is due to temperature-independent contact interaction between the s electrons and the nucleus, and B is a constant that depends on the material. The last term arises from the exchange polarization of the inner s-shell electrons by the d electrons. The d electrons contribute to the temperature-dependent Pauli susceptibility. When we apply an external magnetic field, the d electrons are polarized and attract the inner s-shell electrons of the same polarization, leaving behind antiparallel s electrons. Thus there is a negative contribution to the Knight shift. The exchange interaction is ferromagnetic because parallel spin particles see an "exchange hole" which comes from the antisymmetry requirement of the exclusion principle and, as a result, are less repelled by Coulomb interactions than antiparallel spins.

Finally we can determine the specific heat and susceptibility near $\alpha\simeq 0$ and $y\ll 1$, where the scaling relations become

$$\frac{d\alpha}{dl}\simeq 0\ , \tag{98a}$$

$$\frac{dy}{dl}\simeq y\ . \tag{98b}$$

The solution of these equations is

$$\alpha(l)=\text{const}\simeq 0\ , \tag{99a}$$

$$y(l)=y_0e^{(l-l_c)}=y_0\frac{\tau}{\tau_0}\ . \tag{99b}$$

These describe vertical lines in the y-α plane. Following the same procedure as before, we find

$$C=C_{\text{el}}+\frac{2k_By_0^2\tilde{T}_0^2}{T^2}\ , \tag{100}$$

$$\chi_{\text{Pauli}}=2\mu_B^2N(0)+\frac{6\mu_B^2y_0^2}{\pi^2k_B}\frac{\tilde{T}_0^2}{T^3}\ . \tag{101}$$

In Fig. 7 we show a fit to the susceptibility data of Nb_3Sn.[32] The solid line is given by Eq. (101) with $N(0)=4.3$ states/eV atom, $\tilde{T}_0=2400$ K, and $y_0=1.3\times 10^{-2}$.

For $\alpha\simeq 0,1$ and $y\ll 1$, Eqs. (95) and (100) indicate that the correction to the specific heat due to the local phonon increases as the temperature decreases. This makes sense physically because it simply says that, as the double well becomes shallower with decreasing temperature, the electrons which make the double well deep are less localized and have more degrees of freedom. Thus the specific heat increases. We do not see this happening for $\alpha\simeq 2, y\ll 1$ because the double well is very deep and does not become much shallower until the extremely small Kondo temperature is reached.

How does this compare with traditional electron-phonon perturbation theory? According to Grimvall, $\gamma_1(T)=\gamma(T)-\gamma_{\text{el}}$ has the form shown in Fig. 8 for an Einstein phonon spectrum.[35] At high temperatures Grimvall's $\gamma(T)$ approaches the free-electron value γ_{el}, while at low temperatures, $\gamma(T)=\gamma_{\text{el}}(1+\tilde{\lambda})$, where the conventional electron-phonon coupling

$$\tilde{\lambda}=2\int_0^\infty d\omega\frac{\alpha^2F(\omega)}{\omega}\ .$$

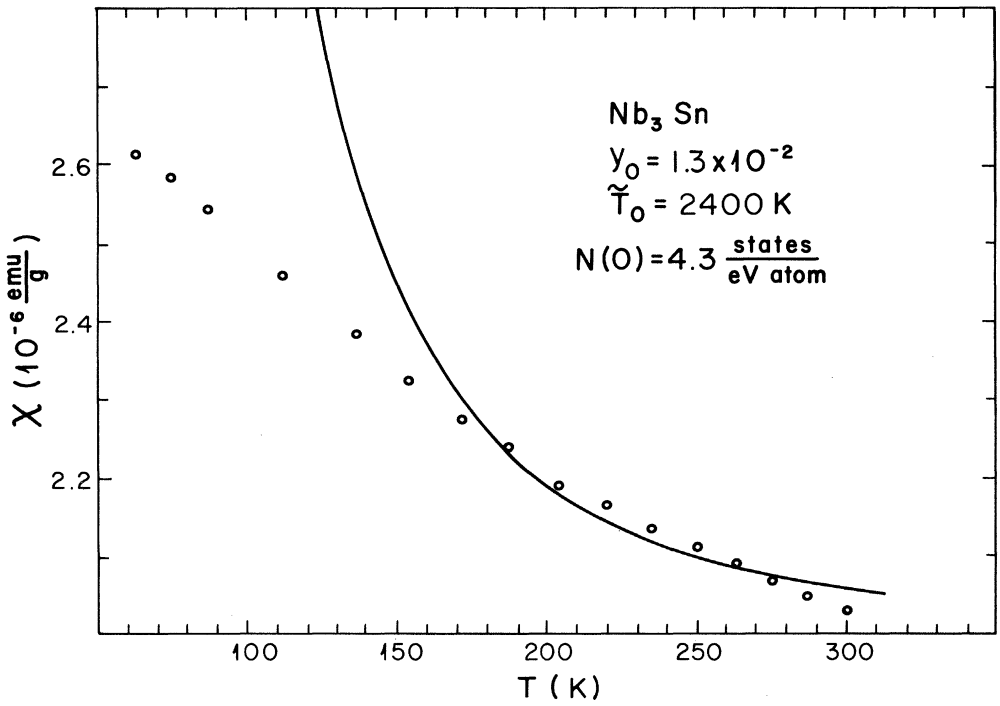

FIG. 7. Fit to the Nb_3Sn susceptibility data of Rehwald *et al.* (Ref. 32).

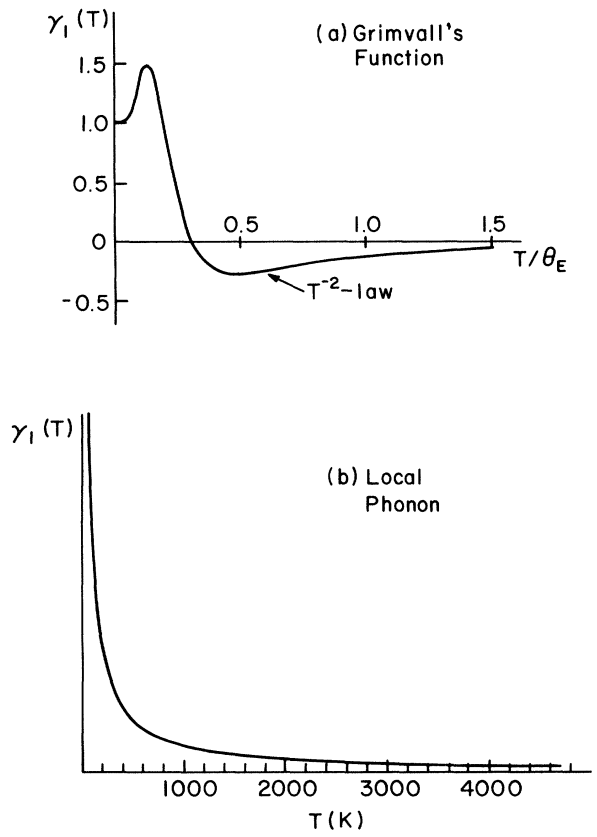

FIG. 8. (a) Grimvall's function $\gamma_1(T)=\gamma(T)-\gamma_{el}$. $\gamma_1(T)$ is normalized to 1 for $T=0$. (b) $\gamma_1(T)$ for the local-phonon model.

For $\alpha\simeq 0,1$ and $y\ll 1$, the local-phonon model predicts that the electron-phonon interaction leads to a specific heat which is greater than the free-electron value. However, Grimvall's result leads to a specific heat which is less than C_{el} for $T>0.3\Theta_E$ where $\Theta_E=\hbar\omega/k_B$ is the Einstein temperature. Grimvall uses a sum-rule argument to explain this. The entropy $S(T)$ is given by

$$S(T)=\int_0^T \frac{C_v}{T'}dT'=\int_0^T[\gamma_0+\gamma_1(T')]dT' =S_0+\int_0^T\gamma_1(T')dT' . \quad (102)$$

Grimvall claims that, for $T\gg\Theta_E$, the electron-phonon interaction is negligible and hence, $S(T)$ approaches S_0 at high temperatures. This implies that the integral in Eq. (102) involving the electron-phonon correction is zero and that the area under the curve in Fig. 8 vanishes. This argument is a bit questionable because it ignores the phonon contribution to the entropy.

VII. RESISTIVITY

Since the phase shift is related to $\alpha(l)$, we can use the scaling relations to find the temperature dependence of the resistivity. With the help of the Boltzmann equation, the conductivity can be expressed approximately as

$$\sigma\simeq-\frac{e^2v_F^2N(0)}{3V}\int d\epsilon\,\tau_1(\epsilon)\frac{\partial f_0(\epsilon)}{\partial\epsilon} , \quad (103)$$

where V is the volume, $f_0(\epsilon)$ is the equilibrium electron distribution, and $N(0)$ is the density of states for one spin and both types of electrons. $\tau_1(\epsilon)$ is the time associated with relaxing back to the equilibrium distribution via scattering.[36] For elastic s-wave scattering,

$$\frac{1}{\tau_1(k)}\simeq\frac{4\pi n_s}{mk}\sin^2\eta_0(k) , \quad (104)$$

where n_s is the density of scatterers, m is the electron mass, and $\eta_0(k)$ is the s-wave phase shift. Elastic scattering is a reasonably good approximation since $\epsilon_F\gg\omega_D$ implies that the electrons basically "see" static phonons and scatter elastically off them. Taking the Fermi function $f_0(\epsilon)$ to be a step function leads to

$$\frac{\partial f_0}{\partial\epsilon}=-2\delta(\epsilon-\epsilon_F) , \quad (105)$$

where the factor of 2 is for spin. Inserting Eqs. (104) and (105) into (103), we obtain, for the resistivity,

$$\rho=\frac{3n_sV^2}{\pi e^2N^2(0)v_F^2}\sin^2\eta_0 . \quad (106)$$

Noting that

$$\alpha=\frac{8}{\pi^2}\eta_0^2 , \quad (107)$$

we can use our solutions to the scaling relations in the vicinity of $\alpha\simeq 2, y\ll 1$ to find the temperature dependence of ρ. In some sense we can view the ρ-versus-T curves as demonstrating the downward renormalization of Λ with decreasing temperature. As we discussed before, we simply scale our cutoff to $l=d(\ln\tau)=d(\ln\beta)$, where the temperature dependence of $\alpha(l)$ and $y(l)$ is $\alpha(\ln\beta)$ and $y(\ln\beta)$. We expand the expression (80a) for $\epsilon(l)$ to lowest order in l/l_0, where $l_0=2\phi/a$ is the point at which $\epsilon(l)$ and $y(l)$ diverge. We assume that $\phi-(a/2)l\ll 1$, which implies that the scaling trajectory is near the separatrix, i.e., $\epsilon(l)\simeq 4y(l)$. We can also assume that a is small such that $a\ll\phi-(a/2)l$. This means that y is small and that the scaling relations are still valid. Then for $l/l_0\ll 1$,

$$\alpha(l)\simeq 2\left[1-\frac{1}{l_0}-\frac{l}{l_0^2}\right] . \quad (108)$$

We would have obtained the same result using Eq. (81a). Expanding $\sin^2\eta_0$ about $\eta_0=\pi/2$ and using Eq. (108), we find that the resistivity depends logarithmically on the temperature,

$$\rho(T)\simeq\rho_0\left[1-\frac{\pi^2}{16l_0^2}+\frac{\pi^2}{8l_0^3}\ln\left[\frac{T}{T_K}\right]\right] , \quad (109)$$

where

$$\rho_0=\frac{3n_sV^2}{\pi N^2(0)e^2v_F^2} . \quad (110)$$

n_s is the density of scatterers, which in this case are local phonons. We take the volume V to be 1 cm^3 and $n_s=5.7\times10^{22}$ vanadium atoms/cm^3. Let the Fermi energy be 1 eV, which corresponds to $v_F\simeq 6\times10^7$ cm/sec.

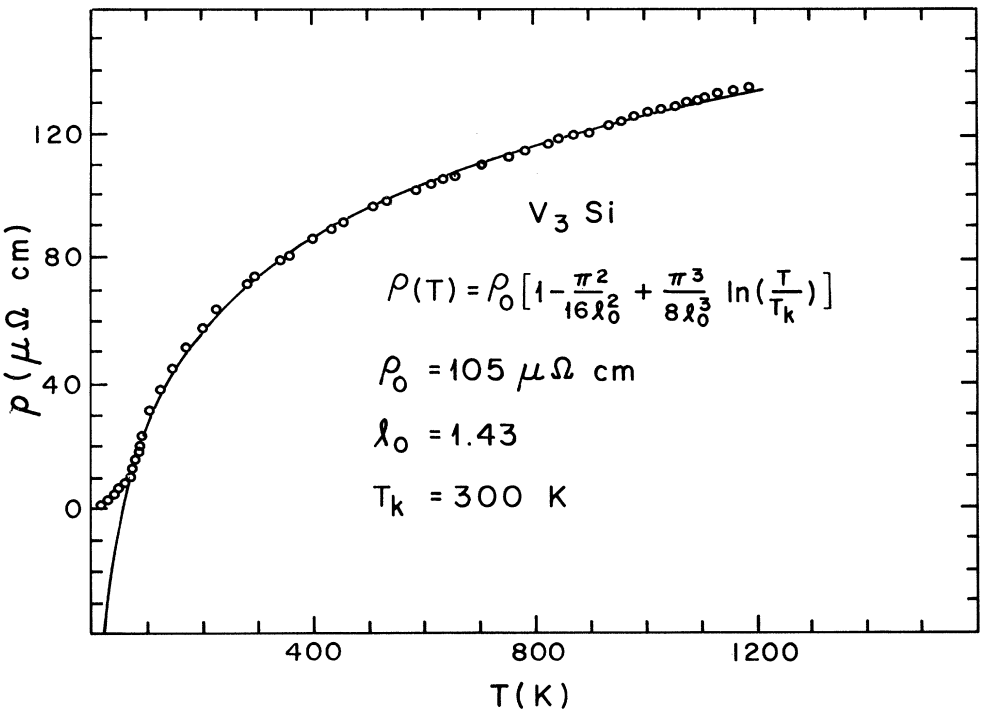

FIG. 9. Logarithmic fit to the V_3Si resistivity data of Marchenko (Ref. 38). The solid line is given by Eq. (109).

The temperature T is measured in units of the Kondo temperature T_K. The above expression for $\rho(T)$ is valid in the vicinity of $\alpha=2$ which corresponds to unitarity limit scattering ($\eta_0=\pi/2$). Most of the electron scattering is off of the quantum rather than the thermal fluctuations of the atom.

Testardi *et al.* have fitted their data for Nb_3Ge and V_3Si with a $\ln T$ function up to 300 K.[37] In Fig. 9 we show a fit to Marchenko's data[38] using Eq. (109) with $T_K=300$ K, $\rho_0=105$ $\mu\Omega$ cm, and $l_0=1.43$. This value of ρ_0 implies that $N(0)=0.7$ states/eV atom according to Eq. (110) since $h/e^2=25\,000$ Ω. Using Eq. (88), we see that $l_0=1.43$ is consistent with $\alpha=0.2$ and $y_0=0.3$. To get α closer to 2, say $\alpha=1.9$, we would need $\rho_0=550$ $\mu\Omega$ cm, $l_0=2.5$, and $T_K=5\times10^6$ K if $y_0=0.3$. Thus it appears that the resistivity of the $A15$ compounds does not have logarithmic temperature dependence.

We can use our solution of the scaling relations in the vicinity of $\alpha=1, y\ll1$ and again determine the temperature dependence of the resistivity. Expanding $\sin^2\eta_0$ about $\eta_1=\pi/2\sqrt{2}$, which corresponds to $\alpha=1$, we obtain, via Eqs. (106), (107), and (94b) with $\tau=\beta$,

$$\rho(T)\simeq\rho_0\sin^2\eta_1\left[1-\sqrt{2}\pi y_0^2\cot\eta_1\left[\frac{1}{\tau_0 T}-1\right]\right]+\rho_1 T\ , \tag{111}$$

where ρ_0 is given by Eq. (110). The linear term has been put in "by hand" to compensate for our neglect of thermal fluctuations. ρ_1 is a parameter to be determined. It is small but not negligible since scattering from quantum fluctuations is not near the unitarity limit. The term which goes inversely with temperature arises from quantum fluctuations.

Figure 10 shows resistivity data for V_3Si (Ref. 38) fitted to a function of the form

$$\rho(T)=A'-\frac{B'}{T}+\rho_1 T\ , \tag{112}$$

where $A'=88$ $\mu\Omega$ cm, $B'=8.1\times10^3$ $\mu\Omega$ cm K, and $\rho_1=4.6\times10^{-2}$ $\mu\Omega$ cm/K. Notice that ρ_1 is at least 3 orders of magnitude smaller than A' and B', which is consistent with our assertion that most of the scattering is from quantum fluctuations in the case of strong electron-phonon coupling. Comparison of Eqs. (111) and (112) yields

$$A'=\rho_0\sin^2\eta_1(1+\sqrt{2}\pi y_0^2\cot\eta_1)\ , \tag{113}$$

$$B'=\sqrt{2}\pi\rho_0\frac{y_0^2}{\tau_0}\sin^2\eta_1\cot\eta_1\ . \tag{114}$$

If $y_0=0.1$, the empirical value of A' implies that $\rho_0=108$ $\mu\Omega$ cm, which is consistent with $N(0)\simeq0.7$ states/eV atom. Using these values, we find that the fit for B' gives $\tilde{T}_0\sim4200$ K.

Woodward and Cody found that the resistivity of Nb_3Sn could be fitted in the range 18–850 K by the function[39]

$$\rho(T)=\rho_a+\rho_0 T+\rho_c\exp\left[-\frac{T_1}{T}\right] \tag{115}$$

where $\rho_a=10$ $\mu\Omega$ cm, $\rho_b=4.66\times10^{-2}$ $\mu\Omega$ cm, $\rho_c=74.7$ $\mu\Omega$ cm, and $T_1=85$ K. Notice that T_1 is on the order of the Kondo temperature. Since the local-phonon model is valid at high temperatures $T\gg T_1$, we can expand the ex-

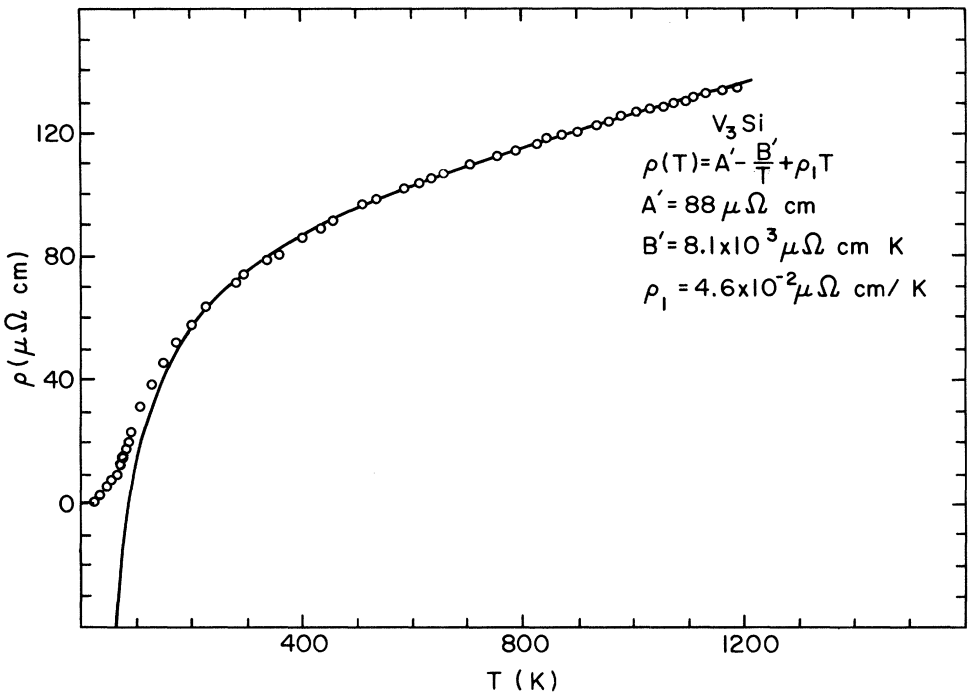

FIG. 10. Another fit to the V_3Si resistivity data of Marchenko (Ref. 38). The solid line is given by Eq. (112).

ponential to lowest order in Eq. (115) to recover Eq. (112). The values of the parameters for Eqs. (112) and (115) are of the same order of magnitude. Fisk and Webb[40] found that Nb_3Sb has the same high-temperature resistivity as Nb_3Sn, which implies that these two compounds have the same bare coupling Λ. However, Nb_3Sb has a much lower T_c ($T_c \sim 0.2$ K) than Nb_3Sn.[41] This would be consistent with Nb_3Sb having a higher Kondo temperature at which it crosses over from strong to weak coupling. A large T_K could result from a large bare stiffness. This is consistent with the observed absence of phonon softening in Nb_3Sb,[41] though the bare stiffness may be as much as 2 orders of magnitude larger than the observable stiffness.

Finally, we can determine the resistivity near $\alpha \simeq 0$ and $y \ll 1$ via the solution to the scaling relations given by Eqs. (99). Since $\alpha \simeq 0$, the phase shift due to quantum fluctuations is roughly zero. Thermal phonons will make a contribution to ρ that is linear in T as we would expect for weak coupling.

VIII. VIOLATION OF MATTHEISSEN'S RULE

The effect of radiation damage on resistivity has been the subject of much experimental and theoretical activity.[2] Mattheissen's rule is clearly violated in that the resistivity curves tend to saturate at high temperatures at roughly the same value (~ 125 $\mu\Omega$ cm) even though the residual resistivity increases with increasing damage. We can simulate the effect of damage by making the Hamiltonian asymmetric in Q, e.g., by adding a term linear in Q to $H_{\rm ph}$ in Eq. (10a),

$$H_{\rm ph}=\frac{P^2}{2M}+\tfrac{1}{2}M\Omega^2Q^2+LQ\ , \tag{116}$$

where L is the asymmetry parameter. Ignoring the quartic term for a moment, we see that this is just the Hamiltonian for a displaced oscillator. We can remove the linear term by completing the square and expressing H in terms of

$$\tilde{Q}=Q+\frac{L}{M\Omega^2}\ . \tag{117}$$

Then

$$H_{\rm ph}=\frac{P^2}{2M}+\tfrac{1}{2}M\Omega^2\tilde{Q}^2\ , \tag{118}$$

where we have dropped the constant term $-L^2/2M\Omega^2$, which simply shifts the energy scale downward. In terms of $\tilde{Q}$, the electron-phonon interaction in Eq. (10c) becomes

$$H_{\text{el-ph}}=-\sum_{\vec{k},\vec{k}'}(c^{\dagger}_{\vec{k}',+}\ c^{\dagger}_{\vec{k}',-})\begin{bmatrix}\lambda\tilde{Q}-\dfrac{\lambda L}{M\Omega^2} & 0\\ 0 & -\left[\lambda\tilde{Q}-\dfrac{\lambda L}{M\Omega^2}\right]\end{bmatrix}\begin{bmatrix}c_{\vec{k}+}\\ c_{\vec{k}-}\end{bmatrix}\ . \tag{119}$$

We can integrate out the fermions just as before and we find the same result as in Eqs. (43)—(45) if we replace Q by $\tilde{Q}$ and γ by $\tilde{\gamma}$, where

$$\tilde{\gamma}=\pi N(0)E(\tilde{Q})=-\pi N(0)\left[\lambda\tilde{Q}-\frac{\lambda L}{M\Omega^2}\right]. \tag{120}$$

Since $\tilde{\gamma}$ does not become $-\tilde{\gamma}$ under the transformation $\tilde{Q}\rightarrow-\tilde{Q}$, the double-well potential $V(\tilde{Q})$ will be asymmetric as shown in Fig. 11. Assuming that there are linear hops between the minima $\tilde{Q}_1$ and $\tilde{Q}_2$, we can do the path integral in much the same way as before. We obtain

$$Z=Z_0\sum_{n=0}^{\infty}e^{-\beta V(\tilde{Q}_1)}\tilde{y}^{2n}\int_0^{\beta}\frac{dt_{2n}}{\tau_0}\int_0^{t_{2n}-\tau_0}\frac{dt_{2n-1}}{\tau_0}\cdots\int_0^{t_2-\tau_0}\frac{dt_1}{\tau_0}\exp\left[\alpha'\sum_{\substack{i,j\\ i>j}}(-1)^{i-j}\ln\left|\frac{t_i-t_j}{\tau_0}\right|-\Delta V\sum_i(-1)^i t_i\right], \tag{121}$$

where

$$\alpha'=2\left[\frac{\tan^{-1}\tilde{\gamma}_2}{\pi}-\frac{\tan^{-1}\tilde{\gamma}_1}{\pi}\right]^2 \tag{122}$$

and

$$\Delta V=V(\tilde{Q}_2)-V(\tilde{Q}_1). \tag{123}$$

The ΔV term in Eq. (121) takes into account the potential energy difference between sitting in the upper well versus sitting in the lower well. Notice that α' reduces to α in the limit $\tilde{\gamma}_2=-\tilde{\gamma}_1=\gamma_0$. The fugacity $\tilde{y}$ is given by

$$\tilde{y}=\exp(S_a+S_b+S_c)\exp\left[-\tfrac{1}{2}M\frac{(\tilde{Q}_2-\tilde{Q}_1)^2}{\tau_0}+A(\tilde{Q}_1,\tilde{Q}_2)\tau_0\right], \tag{124}$$

where

$$A(\tilde{Q}_1,\tilde{Q}_2)=\tfrac{1}{2}\left[\tfrac{1}{6}M\Omega^2(\tilde{Q}_2-\tilde{Q}_1)^2-\frac{1}{\pi N(0)}(\ln|1+\tilde{\gamma}_2^2|+\ln|1+\tilde{\gamma}_1^2|)\right.$$
$$+2\frac{2}{\pi^2N^2(0)\lambda(\tilde{Q}_2-\tilde{Q}_1)}[\gamma_2\ln|1+\tilde{\gamma}_2^2|-\tilde{\gamma}_1\ln|1+\tilde{\gamma}_1^2|$$
$$\left.+2(\tan^{-1}\tilde{\gamma}_2-\tan^{-1}\gamma_1)-2\pi N(0)\lambda(\tilde{Q}_2-\tilde{Q}_1)]\right],$$

$$S_a=-\frac{1}{\pi^2}\ln|\tilde{\gamma}_2-\tilde{\gamma}_1|(\tan^{-1}\tilde{\gamma}_2-\tan^{-1}\tilde{\gamma}_1)^2,$$

$$S_b=\frac{1}{\pi^2}(\tan^{-1}\tilde{\gamma}_2-\tan^{-1}\tilde{\gamma}_1)^2\ln|\tilde{\gamma}_2|+\frac{1}{\pi^2}(\ln|\tilde{\gamma}_2|-\ln|\tilde{\gamma}_1|)\int_{-\tilde{\gamma}_2/\tilde{\gamma}_1}^{-1}dx\left[\frac{1}{1-x^2}\right]\ln\left|\frac{1+\tilde{\gamma}_1^2}{1+\tilde{\gamma}_1^2x^2}\right|$$
$$+\frac{1}{\pi^2}\int_{\tilde{\gamma}_1/\tilde{\gamma}_2}^{1}dx\frac{\ln|1-x|}{1-x^2}\ln\left|\frac{1+\tilde{\gamma}_2^2}{1+\tilde{\gamma}_2^2x^2}\right|-\frac{1}{\pi^2}\int_{-\tilde{\gamma}_2/\tilde{\gamma}_1}^{-1}dx\frac{\ln|1+x|}{1-x^2}\ln\left|\frac{1+\tilde{\gamma}_1^2}{1+\tilde{\gamma}_1^2x^2}\right|,$$

$$S_c=-\frac{P}{2\pi^2}\int_{\tilde{\gamma}_1}^{\tilde{\gamma}_2}d\gamma\,d\gamma'\left[\frac{1}{\tilde{\gamma}^2-\tilde{\gamma}'^2}\ln\left|\frac{1+\tilde{\gamma}^2}{1+\tilde{\gamma}'^2}\right|\right].$$

S_a, S_b, and S_c come from the interaction of a hop with itself. In the symmetric limit, S_b and S_c reduce to Hamann's results,[17]

$$S_b\rightarrow\left[\frac{\tan^{-1}\gamma_0}{\pi/2}\right]^2\ln\gamma_0-\frac{4}{\pi^2}(1.20),$$
$$S_c\rightarrow\ln\gamma_0-\frac{4}{\pi\gamma_0}+\cdots+(\text{const}=0.852), \tag{125}$$

for $\tilde{\gamma}_2=-\tilde{\gamma}_1=\gamma_0$ and $\gamma_0\gg1$. We can find an expression for τ_0 by minimizing the energy of a hopping path:

$$\tau_0=\frac{-\alpha'+[\alpha'^2-8AM(\tilde{Q}_2-\tilde{Q}_1)^2]^{1/2}}{4A}, \tag{126}$$

where $A=A(\tilde{Q}_1,\tilde{Q}_2)$. Knowing that τ_0 minimizes the hopping energy allows us to rewrite the fugacity $\tilde{y}$ as

$$\tilde{y}=\exp(S_a+S_b+S_c)\exp\left[-\frac{M(\tilde{Q}_2-\tilde{Q}_1)^2}{\tau_0}-\frac{\alpha'}{2}\right]. \tag{127}$$

Just as before, we can apply space-time techniques to obtain scaling relations,[18,42]

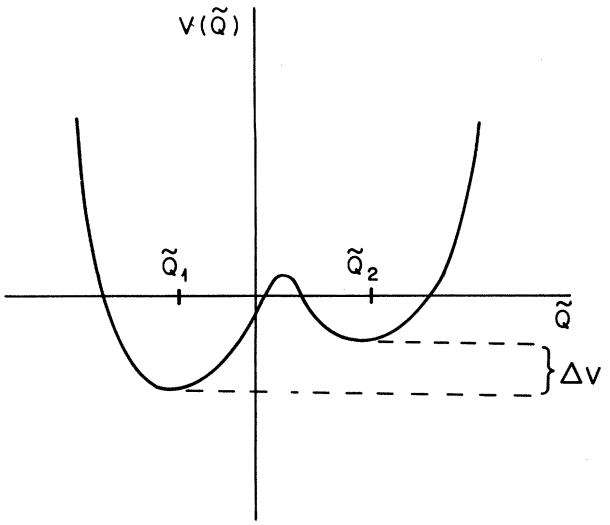

FIG. 11. Asymmetric double-well potential.

$$\frac{d\alpha'}{dl} = -4\alpha'\tilde{y}^2 , \tag{128a}$$

$$\frac{d\tilde{y}}{dl} = \tfrac{1}{2}\tilde{y}(2-\alpha') , \tag{128b}$$

$$\frac{d(\tau\Delta V)}{dl} = (1-2\tilde{y}^2)\tau\Delta V , \tag{128c}$$

where we assumed $\tau\Delta V \ll 1$. If $\tilde{y}_0 \ll 1$, Eq. (128c) implies that the asymmetry initially grows as we proceed along a scaling trajectory. In the α-y plane the scaling trajectories are identical to what we had before. The picture that emerges is one in which the asymmetric double well gradually transforms into a displaced harmonic oscillator potential as $\tilde{y}$ and $\tau\Delta V$ grow. Extended x-ray-absorption fine-structure (EXAFS) measurements of Nb_3Ge indicate that as the damage to the sample is increased, the near-neighbor distance of 2.87 Å splits symmetrically into two distances, 2.77 and 2.97 Å.[43] At $T=0$ we have a displaced single well which is associated with a residual resistivity $\rho(T=0)$ and a phase shift

$$\eta_0 = \tan^{-1}[\pi N(0)\lambda L/M\Omega^2] .$$

At high temperatures, if the trajectory starts near the singularity $\alpha_0 \simeq 2, y_0 \ll 1$, the scattering is very close to the unitarity limit and the resistivity saturates at the same value $\sim\rho_0$, as in the undamaged case. In other words if $(|\eta_1| + |\eta_2|) \simeq \pi/2$, then the resistivity is

$$\rho \simeq \rho_0(\sin^2\eta_1 + \sin^2\eta_2) \simeq \rho_0 , \tag{129}$$

where ρ_0 is given by Eq. (110). This is consistent with the violation of Mattheissen's rule. Notice that the resistivity varies as $(\sin^2\eta_1 + \sin^2\eta_2)$, whereas $\alpha' \sim (|\eta_1| + |\eta_2|)^2$ is the quantity which scales. The resistivity does not vary as

$$\sin^2(|\eta_1| + |\eta_2|)/2$$

because the atom cannot be in both minima at once. Such an expression would imply that there are interference effects.

IX. QUANTUM COHERENCE

The scaling relations imply that, if the system initially has very strong coupling, the double well will be reasonably deep and the local phonon will be anharmonic at high temperatures. As the temperature decreases, the double well becomes shallower and the fugacity increases, indicative of anomalously large zero-point motion. This is consistent with the well-documented experimental evidence for anharmonic phonons[1] and for anomalously large zero-point motion. X-ray measurements indicate anharmonic motion of the vanadium atom in V_3Si and a tendency for V atoms to localize ~ 0.1—0.2 Å off the lattice sites at 78 K.[4]

The reason why the ground state can be associated with infinite fugacity is best understood within the context of quantum coherence. Recently, there has been interest in the problem of quantum tunneling and quantum coherence with dissipation.[42,44–47] "Quantum tunneling" refers to an atom coupled to other phonons which is trying to tunnel out of a single well. "Quantum coherence" refers to an atom coupled to other phonons which is trying to tunnel between two wells in a double-well potential. If we go back to our Tomonoga-boson Hamiltonian (3) and introduce canonically conjugate-coordinate and momentum operators

$$Q_{\vec{k}} = \left[\frac{1}{2\Omega_k}\right]^{1/2}(a_{\vec{k}} + a^\dagger_{-\vec{k}}) ,$$

$$P_{\vec{k}} = -i\left[\frac{\Omega_k}{2}\right]^{1/2}(a_{\vec{k}} - a^\dagger_{-\vec{k}}) , \tag{130}$$

$$q = \left[\frac{1}{2\omega_0}\right]^{1/2}(b + b^\dagger),\quad p = -i\left[\frac{\omega_0}{2}\right]^{1/2}(b - b^\dagger) ,$$

then the Hamiltonian is essentially the same as that used by Caldeira and Leggett,[45] and Bray and Moore.[44] Namely,

$$H = \tfrac{1}{2}\sum_{\vec{k}}(P^*_{\vec{k}}P_{\vec{k}} + \Omega_k^2 Q^*_{\vec{k}}Q_{\vec{k}}) + \tfrac{1}{2}(p^*p + \omega_0^2 q^*q) + \tfrac{1}{2}\sum_{\vec{k}} C_k(Q^*_{\vec{k}}q + Q_{\vec{k}}q^*) , \tag{131}$$

where $C_k = \Lambda\Omega_k\omega_0/4\pi^{1/2}$. Our Tomonoga bosons are the phonons of Caldeira and Leggett (CL). CL deliberately added a counterterm to their Hamiltonian to cancel the softening of the local phonon, and then manually inserted a double-well or a single-well potential $V(Q)$. Using path-integral techniques, they integrated out the Tomonoga bosons. Chakravarty,[42] and Bray and Moore,[44] applied space-time scaling techniques and found that if the viscosity η was large enough ($\eta > 2$), they could map their problem onto the ferromagnetic Kondo problem. Since η is related to the coupling constant C_k, this means that if the coupling is sufficiently strong, the atom gets stuck in one well and the symmetry is broken.

Why do they find symmetry breaking whereas we do not? The basic reason is that their atom is coupled to boson degrees of freedom, whereas ours is coupled to fermion degrees of freedom. Consider the bose case first. If the coupling is sufficiently strong, the atom can pull all

the bosons into the vicinity of one well where they are able to bose-condense. Thus the fugacity goes to zero at $T=0$ if $\eta>2$. In the case of fermions, the Pauli exclusion principle does not allow enough electrons to pile into one well and to make it so deep that the atom gets stuck. At $T=0$, the ground-state wave function is symmetric and the atom has an equal probability of being in either well. Equivalently, the double well has become a single well. Either way, the fugacity flows into the $y=\infty$ fixed point as the temperature goes to zero. If there were more kinds of electrons, then the local charge density in the neighborhood of one well would be sufficiently large to trap the atom. We can map the fermion case onto the ferromagnetic Kondo problem and obtain self-trapping of the atom by merely adding spin to the problem. If we ignore U terms and simply introduce two spin species, then α is doubled and the coefficient of the anharmonic term in the effective potential of Eq. (44) becomes $2/\pi N(0)$. We now have $0\leq 2\alpha\leq 4$. In the range $0\leq 2\alpha\leq 2$, the fugacity scales to infinity and the double well disappears as the temperature decreases. For $2\leq 2\alpha\leq 4$, the fugacity scales to zero and the atom becomes trapped in one well. But this is a moot point; even without spin, if the coupling is so strong that $1\leq\alpha\leq 2$, the fugacity is so low that the atom is stuck until the temperature is on the order of T_K, which is very small. This is consistent with Nozières and Blandin who have argued that the Kondo system scales to a finite coupling if $n>2S$, where n is the number of orbital channels of the conduction electrons and S is the spin of the impurity.[48] Their arguments have been confirmed by numerical calculations and the exact solution.[49,50]

X. MARTENSITIC TRANSITION

The fact that the flipping fugacity scales from small to large explains why the martensitic transition, if it occurs at all, occurs at such low temperatures ($T_m \ll \Theta_D$) and with such small lattice displacement ($Q_m \sim 0.005$ Å $\ll Q_{\text{thermal}} \sim 0.1$ Å), even though there are anharmonic effects at $T\sim\Theta_D$.[1] The martensitic transition corresponds to the softening of an acoustic shear mode, but the crystal structure of the $A15$ compounds couples this acoustic mode to the optic mode associated with our Einstein oscillator.[51] We can write a schematic form for the Hamiltonian,

$$H\sim\sum_{\vec{k}}\tfrac{1}{2}\omega_0^2 Q_{\vec{k}}^2+\tfrac{1}{2}\sum_{\vec{k}}k^2c^2\delta_{\vec{k}}^2+\sum_{\vec{k}}gk\delta_{\vec{k}}Q_{\vec{k}}\ , \tag{132}$$

where $Q_{\vec{k}}$ is the optic-mode displacement, ω_0 is the optic-phonon frequency, c is the speed of sound, $\delta_{\vec{k}}$ is the acoustic-mode displacement, and g is the coupling between these modes. We can diagonalize this Hamiltonian by choosing the appropriate linear combinations of $Q_{\vec{k}}$ and $\delta_{\vec{k}}$. The point is that the "new" acoustic mode which undergoes the martensitic transition has the "old" local-phonon mode mixed into it.

As we have shown, strong electron-phonon coupling leads to an effective double-well potential and anharmonic phonons. Without the kinetic term in the Hamiltonian to describe hopping between the wells, we would predict a large displacive transition occurring at a rather high transition temperature. But, with the kinetic term of Eq. (45), the depth of wells diminishes with decreasing temperature. Thus the kinetic term causes the transition temperature to be lowered and the lattice displacement to be reduced. This picture has some features in common with McMillan's theory of phonon entropy in which the thermal fluctuations of the phonons, rather than quantum fluctuations, cause the transition temperature to be lower than that predicted by mean-field theory.[52] Varma and Simons have recently extended McMillan's idea to include anharmonic phonons and strong electron-phonon coupling.[53]

XI. CONCLUSIONS

In this paper we have examined a local-phonon model in which a single atom interacts strongly with a Fermi gas of spinless electrons. By integrating out the electrons, we found that strong coupling leads to anharmonic phonons. In particular, the electrons provide an effective double-well potential for the atom as well as time-retarded interactions between hops from one minimum to the other. Such time-retarded interactions reveal the breakdown of the adiabatic approximation and of Migdal's theorem due to strong coupling. Using space-time scaling techniques, we found that if the electron-phonon coupling is large at high temperatures, it is renormalized downwards. The crossover from the region dominated by the strong-coupling fixed point to that dominated by the weak-coupling fixed point occurs at $T_K\sim 90$ K. The fugacity scales upward and the phase shift scales downward as the temperature decreases. This implies that the double well becomes shallower and eventually transforms into a single well. The ground state is symmetric and the atom does not get stuck in one of the double-well minima, no matter how strong the coupling if the electrons have no spin.

By expanding the partition function to lowest order in the fugacity, we found a temperature-dependent density of states for $\alpha\lesssim 1$ which is consistent with the experimental data on the temperature dependence of the Pauli susceptibility for $T\gtrsim\Theta_D$. The scaling relations for the phase shift implied that the resistivity goes logarithmically with the temperature if $\alpha_0\sim 2$ and $y_0\ll 1$ as in Eq. (109). If $\alpha_0\sim 1$ and $y_0\ll 1$, the high-temperature resistivity varies as $\rho_1 T-B/T$ according to Eq. (112). Both of these cases can be fitted to the experimental data. However, numerical estimates indicate α_0 is closer to 1 than to 2. In the numerical estimates the intrinsic stiffness of the harmonic-oscillator potential was large. This was needed to prevent the phonon from becoming soft due to the strong electron-phonon coupling. By introducing a symmetry-breaking term LQ into our Hamiltonian to mimic the effect of damage on a sample, we found that our model is consistent with the violation of Mattheissen's rule. If the scattering from quantum fluctuations of the atom is near the unitarity limit, i.e., if $\alpha_0\sim 2$, then the resistivity of the damaged and undamaged samples saturates at the same value ρ_0, even though the residual resistivity of these samples is different.

The fact that the flipping fugacity scales toward $y=\infty$ as the temperature decreases explains why the martensitic transition has such small lattice displacements and occurs at such low temperatures even though there are phonon anharmonicities at much higher temperatures. Strong

electron-phonon coupling leads to anharmonic phonons and an effective double-well potential. Normally, we would expect that lowering the temperature would cause the atom to get stuck in one well. This corresponds to a displacive transition. But as the temperature decreases, the hopping fugacity increases and the double well becomes shallower, thus preventing a transition from occurring. It should be interesting to probe such a high-temperature double well via x-ray-diffraction and EXAFS techniques. A crucial experiment is to show that the Debye-Waller factors are anomalously large at $T=0$ compared to the Debye prediction.

Note added in proof. This concerns Eq. (40). Another way to handle the divergence of the adiabatic part of the Green's function in Eq. (40) is to solve Dyson's equation for a constant potential. This leads to an effective potential which has the same functional form as the Anderson model in Eq. (53).[54]

ACKNOWLEDGMENTS

We would like to thank I. Affleck, C. Bachas, R. N. Bhatt, M. C. Cross, T. H. Geballe, M. Gurvitch, B. G. Kotliar, J. P. Sethna, and A. Z. Zawadowski for helpful discussions. We thank the Aspen Center for Physics for its hospitality. The work done at Princeton University was supported in part by National Science Foundation grant No. DMR-80-20263.

APPENDIX

In this appendix we show that a δ-function potential at the origin

$$V(r)=\lambda Q_0\delta(r) \tag{A1}$$

gives an s-wave phase shift of

$$\eta_0=-\tan^{-1}[\pi N(0)\lambda Q_0] \tag{A2}$$

to the electron wave function at the Fermi surface.

We start with the wave function

$$\psi_{\vec{k}}(\vec{r})=\frac{1}{kr}\sum_l \chi_l(r)P_l(\cos\theta)\ , \tag{A3}$$

where the $l=0$ component of the radial part satisfies

$$\left[-\frac{d^2}{dr^2}+U(r)-k^2\right]\chi_0(r)=0\ . \tag{A4}$$

Here,

$$U(r)=2mV(r)$$

and

$$k^2=2mE\ .$$

If the potential falls off more rapidly than r^{-1}, $\chi(r)$ satisfies the boundary conditions

$$\chi(0)=0,\quad \lim_{r\to\infty}\chi(r)=\sin(kr)+\tan\eta\cos(kr)\ . \tag{A5}$$

Following Kohn,[21] we introduce the sine transform

$$\chi(r)=\int_0^\infty dp\,\chi(p)\sin(pr)\ , \tag{A6}$$

$$U_{pp'}=\int_0^\infty dr\sin(pr)U(r)\sin(p'r)\ . \tag{A7}$$

Then we obtain

$$(p^2-k^2)\chi_0(p)+\int_0^\infty dp'\chi_0(p)U_{p'p}=0\ . \tag{A8}$$

The singularity behavior of $\chi_0(p)$ can be expressed by

$$\chi_0(p)=\delta(p-k)-\frac{B(k)}{2k}\frac{1}{p-k}\ , \tag{A9}$$

where we have neglected regular terms which vanish as $x\to\infty$. $B(p)$ is a nonsingular function given by

$$B(p)=\int_0^\infty dp'U_{pp'}\chi_0(p')\ . \tag{A10}$$

Transforming χ_0 back to coordinate space and using

$$\mathrm{P}\int_0^\infty \mathrm{d}p\frac{\sin(px)}{p-k}\to\pi\cos(kx)\ \text{ as } x\to\infty\ ,$$

we find the phase shift to be

$$\eta=-\frac{\pi B(k)}{2k}\ . \tag{A11}$$

Near the Fermi surface, $\epsilon_k\simeq v_F\,|\,\vec{k}\,|$, so that (A9) becomes

$$\chi_0(p)=v_F\delta(\epsilon_p-\epsilon_k)+\frac{v_F\tan\eta}{\pi}\frac{1}{\epsilon_p-\epsilon_k}\ . \tag{A12}$$

Substituting (A10) and (A12) into (A11), we have

$$\tan\eta=-\pi N(0)\int_{-\infty}^\infty d\epsilon_{p'}V_{pp'}\left[\delta(\epsilon_{p'}-\epsilon_k)+\frac{1}{\pi}\tan\eta\,\mathrm{P}\left[\frac{1}{\epsilon_{p'}-\epsilon_k}\right]\right]\ , \tag{A13}$$

where P denotes principal value. In our case, $V_{pp'}=\lambda Q_0=\text{const}$. Thus the second term in (A13) vanishes and we finally obtain

$$\tan\eta_0=-\pi N(0)\lambda Q_0\ . \tag{A14}$$

---

[1]There are several good review articles: M. Weger and I. B. Goldberg, in *Solid State Physics: Advances in Research and Applications,* edited by F. Seitz and D. Turnbull (Academic, New York, 1973), Vol. 28, p. 1; Yu. A. Izyumov and Z. Z. Kurmaev, Usp. Fiz. Nauk. 113, 193 (1974) [Sov. Phys.—Usp. 17, 356 (1974)]; L. R. Testardi, *Physical Acoustics* (Academic, New York, 1973), Vol. 10, p. 193; L. R. Testardi, Rev. Mod. Phys. 47, 637 (1975); J. Muller, Rep. Prog. Phys. 43, 641 (1980).

[2]See, for example, R. Caton and R. Viswanathan, Phys. Rev. B 25, 179 (1982), and references therein.

[3]L. R. Testardi, J. M. Poate, W. Weber, and W. M. Augustyniak, Phys. Rev. Lett. 39, 716 (1977).

[4]J. L. Staudenmann and L. R. Testardi, Phys. Rev. Lett. 43, 40

(1979).
[5]L. R. Testardi and T. B. Bateman, Phys. Rev. 154, 402 (1967).
[6]G. R. Steward, in *Superconductivity in d- and f-Band Metals,* edited by W. Buckel and W. Weber (Kernforschungszentrum Karlsruhe, Karlsruhe, West Germany, 1982), p. 81.
[7]A. M. Clogston and V. Jaccarino, Phys. Rev. 121, 1357 (1961).
[8]L. R. Testardi, Phys. Rev. B 5, 4342 (1972).
[9]L. P. Gor'kov, Zh. Eksp. Teor. Fiz. 65, 1658 (1973) [Sov. Phys.—JETP 38, 830 (1974)]; L. P. Gor'kov and O. N. Dorokov, J. Low Temp. Phys. 22, 1 (1976).
[10]See, for example, *Ternary Superconductors,* edited by G. K. Shenoy, B. D. Dunlap and F. Y. Fradin (North-Holland, New York, 1981).
[11]S. Tomonoga, Prog. Theor. Phys. 5, 544 (1950).
[12]S. Engelsberg and B. B. Varga, Phys. Rev. 136A, 1582 (1964).
[13]A. B. Migdal, Zh. Eksp. Teor. Fiz. 34, 1438 (1958) [Sov. Phys.—JETP 37, 996 (1958)].
[14]P. W. Anderson, Phys. Rev. 124, 41 (1961).
[15]A good review is M. D. Sturge, in *Solid State Physics: Advances in Research and Applications,* edited by F. Seitz and D. Turnbull (Academic, New York, 1967), Vol. 20, p. 91.
[16]G. Yuval and P. W. Anderson, Phys. Rev. B 1, 1522 (1970).
[17]D. R. Hamann, Phys. Rev. B 2, 1373 (1970).
[18]P. W. Anderson, G. Yuval, and D. R. Hamann, Phys. Rev. B 1, 4464 (1970).
[19]P. Nozières and C. De Dominicis, Phys. Rev. 178, 1097 (1969).
[20]N. I. Muskhelishvili, *Singular Integral Equations,* translated by J. R. M. Radok (Nordhoff, Leyden, The Netherlands, 1977).
[21]W. Kohn, Phys. Rev. 84, 495 (1951).
[22]M. C. M. O'Brien, Proc. R. Soc. London, Ser. A 281, 323 (1964).
[23]J. E. Jorgensen, J. D. Axe, L. M. Corliss, and J. M. Hastings, Phys. Rev. B 25, 5856 (198). Γ_2 and Γ_{12} are longitudinal-optical phonon modes.
[24]P. W. Anderson, J. Phys. C 3, 2436 (1970).
[25]A. P. Young and T. Bohr, J. Phys. C 14, 2713 (1981).
[26]K. G. Wilson, Phys. Rev. B 4, 3174 (1971).
[27]I. Affleck, Phys. Rev. Lett. 46, 388 (1981).
[28]P. W. Anderson and C. C. Yu, in Proceedings of the International School of Physics "Enrico Fermi" (Varenna, Italy, 1983) (to be published).
[29]G. S. Knapp, S. D. Bader, H. V. Culbert, F. Y. Fradin, and T. E. Klippert, Phys. Rev. B 11, 4331 (1975).
[30]G. S. Knapp, S. D. Bader, and Z. Fisk, Phys. Rev. B 13, 3783 (1976).
[31]J. P. Maita and E. Bucher, Phys. Rev. Lett. 29, 931 (1972).
[32]W. Rehwald, M. Rayl, R. W. Cohen, and G. D. Cody, Phys. Rev. B 6, 363 (1972).
[33]G. W. Webb, Z. Fisk, and D. C. Johnston, Phys. Lett. 73A, 350 (1979).
[34]W. E. Blumberg, J. Eisinger, V. Jaccarino, and B. T. Matthias, Phys. Rev. Lett. 5, 149 (1960).
[35]G. Grimvall, J. Phys. Chem. Solids 29, 1221 (1968).
[36]See, for example, G. D. Mahan, *Many-Particle Physics* (Plenum, New York, 1981), pp. 592—597.
[37]L. R. Testardi, J. M. Poate, and H. J. Levinstein, Phys. Rev. B 15, 2570 (1977).
[38]V. A. Marchenko, Fiz. Tverd. Tela (Leningrad) 15, 1893 (1973) [Sov. Phys.—Solid State 15, 1261 (1973)].
[39]D. W. Woodward and G. D. Cody, Phys. Rev. 136, A166 (1964).
[40]Z. Fisk and G. W. Webb, Phys. Rev. Lett. 36, 1084 (1976).
[41]L. Pintschovius *et al.*, in *Superconductivity in d- and f-Band Metals,* Ref. 6, p. 9.
[42]S. Chakravarty, Phys. Rev. Lett. 49, 681 (1982).
[43]G. S. Knapp, R. T. Kampwirth, P. Georgopoulos, and B. S. Brown, in *Superconductivity in d- and f-Band Metals,* edited by H. Suhl and M. B. Maple (Academic, New York, 1980), p. 363.
[44]A. J. Bray and M. A. Moore, Phys. Rev. Lett. 49, 1545 (1982).
[45]A. O. Caldeira and A. J. Leggett, Phys. Rev. Lett. 46, 211 (1981).
[46]V. Ambegaokar, V. Eckern, and G. Schön, Phys. Rev. Lett. 48, 1745 (1982).
[47]J. P. Sethna, Phys. Rev. B 24, 698 (1981); J. P. Sethna, *ibid.* 25, 5050 (1982).
[48]P. Nozières and A. Blandin, J. Phys. (Paris) 41, 193 (1980).
[49]D. M. Cragg, P. Lloyd, and P. Nozières, J. Phys. C 13, 803 (1980).
[50]A. M. Tsvelick and P. B. Wiegmann, J. Phys. C (to be published); N. Andrei and C. Destri, Phys. Rev. Lett. 52, 364 (1984).
[51]R. N. Bhatt and W. L. McMillan, Phys. Rev. B 14, 1007 (1976); R. N. Bhatt, *ibid.* 17, 2947 (1978).
[52]W. L. McMillan, Phys. Rev. B 16, 643 (1977).
[53]C. M. Varma and A. L. Simons, Phys. Rev. Lett. 51, 138 (1983); C. M. Varma (unpublished).
[54]L. D. Chang and S. Chakravarty (unpublished).